HHS Public Access

Author manuscript

Colloids Surf B Biointerfaces. Author manuscript; available in PMC 2020 February 01.

Published in final edited form as:

Colloids Surf B Biointerfaces. 2019 February 01; 174: 232–245. doi:10.1016/j.colsurfb.2018.11.018.

pH Responsive 5-Fluorouracil Loaded Biocompatible Nanogels For Topical Chemotherapy of Aggressive Melanoma

Prashant Sahu[a], **Sushil K. Kashaw**[a,b,*], **Samaresh Sau**[b,*], **Varun Kushwah**[c], **Sanyog Jain**[c], **Ram K. Agrawal**[a], **Arun K. Iyer**[b,d,*]

[a]Department of Pharmaceutical Sciences, Dr. Harisingh Gour University (A Central University), Sagar, MP, India

[b]Use-inspired Biomaterials & Integrated Nano Delivery (U-BiND) Systems Laboratory, Department of Pharmaceutical Sciences, Wayne State University, Detroit, Michigan, USA

[c]Centre for Pharmaceutical Nanotechnology, Department of Pharmaceutics, National Institute of Pharmaceutical Education and Research (NIPER), Sector 67, SAS Nagar Mohali, Punjab, India

[d]Molecular Imaging Program, Karmanos Cancer Institute, Detroit, Michigan, USA

Abstract

Combating melanoma via topical route is a highly challenging task due to low selectivity, poor efficacy and impeding biological environment of the skin. In the present study, we engineered a chitosan based pH responsive biodegradable nanogel (FCNGL), encapsulated with 5-FU that was effective even at very low drug doses (0.2% w/v) against melanoma. The FCNGL was synthesized by ion gelation technique exhibited nano-size particle distribution and sustained drug release kinetics. Hemolysis and coagulation analysis revealed high safety whereas MTT and apoptosis assays exhibited the efficacy of FCNGL. DMBA-Croton oil Swiss albino mice model was employed for in vivo assessment followed by gamma scintigraphic screening. Tumor burden and pharmacokinetic antioxidant stress levels along with whole-body gamma scintigraphy imaging using 99 mTc labelled nanogel exhibited selective accumulation in melanoma tumor nodules. The pH responsive behaviour of the nanogels resulted in triggered release of 5-FU in slightly acidic microenvironment, resulting in selective drug accumulation at the melanoma site. Immunohistochemistry (IHC) analysis of tumor showed improvement of subcutaneous layer alignment and regeneration of the epithelial skin layer when compared with standard 5% 5-FU and control mice group. Overall our preclinical data using the FCNGL portends to be a promising platform for efficient and sustained delivery of 5-FU for topical chemotherapy that can result in high efficacy, patient compliance and safety in the clinical set up.

*Corresponding authors. sushilkashaw@gmail.com (S.K. Kashaw), samaresh.sau@wayne.edu (S. Sau), arun.iyer@wayne.edu (A.K. Iyer).

6. Disclosure

The authors declare no conflict of interest associated with the manuscript.

Appendix A. Supplementary data

Supplementary material related to this article can be found, in the online version, at doi:https://doi.org/10.1016/j.colsurfb.2018.11.018.

Keywords

Biodegradable chitosan nanogel; topical chemotherapy; pH responsive drug release; 5-FU; Gamma scintigraphy; melanoma

1. Introduction

Melanoma is one of the deadliest skin cancer that accounts for about 80% of mortality rates with severe metastasis property[1]. It is referring to the cancer that arises from melanocytes and spreads to the other part of the skin tissue rapidly. Combating melanoma is challenging due to its highly invasive, metastasis and heterogeneous nature, thus it is required multimodal treatments, which includes chemotherapy, radiation therapy, surgery, and photodynamic therapy [2,3]. Despite great progress in current therapies, there is still lack of new modalities that can completely eradicate melanoma.

Skin cancer cases are more prominent in white population as compare to brown or black population. The ratio of melanoma occurrence in black population compare to white is 1:10 whereas in brown skin peoples, the ratio increases to 3:10 [4,5]. Melanoma appears in the skin as black, brown lumps or wart type structures and in some cases, do not produce melanin lumps and arises as pink, tan or white lumps [6]. Currently, the rate of occurrence of melanoma is increasing at an alarming rate where it is not restricted to the certain areas of the body but also appear anywhere including eyes, genital organs and feet of both genders [7]. Since melanoma is one of the fast metastasizing cancer among epithelial tumors, early diagnosis is an urgent need for initiating the treatment at early stages to achieve prognostic therapy response[8].

For combating melanoma, numerous treatment strategies have been introduced along with the existing techniques such as molecule targeting [9], photodynamic therapy [10], gene therapy and nanotechnology[11]. Currently in the clinical setting, chemotherapy, radiation therapy, and immunotherapy based on check point inhibitors (anti-PD-1/PDL-1) are the first line approaches for melanoma patients [12]. The above mentioned therapeutic approaches are much costlier and cannot be afforded by every patient, therefore, there must be a rational approach to develop low cost but efficient drug delivery agent for deadliest melanoma[13,14]. With the advancement of nanotechnology and drug delivery systems, treatment of melanoma has been diversified. In this regard nanogel is a promising and cost-effective option, especially for topical chemotherapeutic delivery [15].

Topical administration is the second most preferable route for drug delivery as it provides advantages of self-medication, bypasses first pass metabolism, painless therapy and ultimately offers patient compliance with high level of safety. For the last few decades the advancement of nanotechnology based topical drug delivery system has received increasing attention for treating highly metastatic melanoma [16,17,18]. Current topical treatment includes delivery of drugs to the epithelial cells in which the therapeutic efficiency is restricted on dermal region, yielding marginal therapeutic benefit. In this regard, Efudex 5% and 2%, and Fluoroplex 1% w/v are only available topical gels that have been utilized in clinic against SCC and BCC for more than few decades, with limited therapeutic value

against melanoma [19]. Thus, there is a requirement of developing more potent and biocompatible topical formulation for treatment of melanoma.

5-FU, an antineoplastic pyrimidine analogue has been utilized for colon, oesophageal, pancreatic cancer and carcinomas. It's function as an antimetabolite agent is mediated through blocking the action of thymidylate synthase, thus inhibiting DNA synthesis [20]. Treatment with conventional 5-FU gel of melanoma is a challenging task due to its complicated biological environment [21] and low tissue penetration of macro-sized gels particles [22]. The absorption of large amount of 5-FU in the upper layer is high whereas the cytotoxic effects of 5-FU in deeper embedded melanoma cells remains low [23]. Usually, FDA approved 5-FU topical gel are applied twice a day for 2–4 weeks duration that leads to noticeable side effect such as lysis of blood cells, hair loss, erythema, oedema and severe local skin eruptions [24].

Current drug development strategies include "repurposing of existing drugs" as a plausible option by formulating them in sustained and biodegradable nano-system for target specific delivery that would reduce the time and cost of new drug development for clinical use [25,26,27]. Towards this end, we engineered 5-FU encapsulated biodegradable chitosan nanogels (FCNGL) for topical chemotherapy (Fig. S1).

2. Materials and Method

2.1. Materials

Chitosan of medium molecular weight (medical grade) with degree of de-acetylation 75%, hydrochloric acid (HCl) and Acetic acid 100% ultra-pure was procured from Hi-media chemical Ltd Mumbai, India. Sodium tri-polyphosphate (TPP), Technetium-99 m, stannous chloride dehydrate and Pluronic F-127 (PF-127) were purchased from Sigma Aldrich, Bengaluru, India. Bulk drug 5-FU was procured as a benevolent gift from Taj Pharmaceutical Pvt. Ltd, Hyderabad, India. Phosphotungstic acid (PTA), chloroform, ethyl acetate, sodium bicarbonate ($NaHCO_3$) and sodium chloride (NaCl) were purchased from Rankem Chemicals Ltd, New Delhi India. Deionized water was produced from Milli-Q Synthesis (18 MΩ, Millipore). All other reagents and chemical were of analytical grade and used as received.

2.2. Fabrication of 5-FU-Chitosan Biodegradable Nanogel (FCNGL)

Ion gelation technique was employed for the fabrication of 5-FU loaded nanogel (FCNGL) system with the aid of PF-127. 5-FU loaded chitosan nanogel (FCNGL) was synthesized by addition of about 100 mg of Fluorouracil and 0.4% w/v of chitosan dissolved in 1% v/v aqueous acetic acid solution followed by the drop wise addition of 0.4% TPP at the rate of 2 ml/min with constant stirring for 2 h by using magnetic stirrer at 500 rpm (REMI, New Delhi). The resulting drug loaded particles dispersion were processed using probe sonicator (S-4000; Misonix, Farmingdale, NY) at medium amplitude (50%) for 5 min to arrive FCNGL of size less than 200 nm. The dispersion was finally filtered through a 1.2 μm hydrophilic filter (Minisart, Sartorius) [28]. The FCNGL particles were thoroughly purified by ultrafiltration (Amicon 8200 with a Millipore PBMK membrane, MWCO 30 kDa)

against double distilled water at ambient temperature to remove the remaining unreacted solvent and elimination of unreacted drug. The obtained 5-FU nanoparticles were added in 22% w/v PF-127 aqueous solution in magnetic stirrer (REMI, New Delhi) for about 2 h at 1000 rpm for the final synthesis of biodegradable 5-FU chitosan nanogel system (FCNGL) retained overnight at 25 °C of temperature undisturbed after efficient dissolving PF-127 in distilled water. The prepared nanogel was kept at ambient temperature for further use (Fig. S2) [29].

3. Characterizations of FCNGL

3.1. Particle Size, Poly-dispersity Index (PDI), Zeta potential and Morphology

The particle size, surface charge and PDI of FCNGL were assessed by Malvern Zetasizer 3000 (Malvern Instruments, Bedfordshire, UK). The Zeta potential of FCNGL was evaluated by using the principle of electrophoretic mobility of particles in an applied electrical field. The concentration of developed nanogel was adjusted to 0.01% w/v using distilled water or in 0.01 M sodium chloride solution for potential assessment [30]. The formulation analysis was triplicated and average of triplicated data along with SD was reported.

3.2. Transmission Electron Microscopy (TEM)

TEM (Transmission electron Microscopy) of FCNGL was performed using Hitachi H-7500 TEM instrument. TEM images were evaluated to visualize the shape and structure of FCNGL. The FCNGL formulation was coated with 2.5% w/v of Phosphotungstic acid (PTA) solution and placed in a copper grid. The grid was then dried in 60 watt LED lamp (Philips, India Ltd) and was finally placed into the disc holder and scanned for transmission electron microscopy analysis [31].

3.3. Scanning Electron Microscopy (SEM)

From the structural point of view, the arrangement, morphology and orientation of developed FCNGL was assessed by scanning electron microscopy (SEM), Nova Nano SEM 450, Germany. Prior to the SEM evaluation the FCNGL formulation was lyophilised by using lyophilization, REMI, New Delhi, India. The freeze-dried FCNGL nanoformulation was placed on SEM stub by employing double sided adhesive tape at 50 mA for 5–10 min for gold sputter coating (KYKY SBC-12, Beijing, China)[32]. A scanning electron microscope aided with secondary electron detector was employed to obtain digital images of the developed FCNGL.

3.4. Dynamic Light Scattering (DLS)

The FCNGL nanoformulation was further subjected to DLS for the advanced evaluation of mean diameter and PDI using Brook-heaven BI 9000 A T instrument system (Brookhaven Instrument Corporation, USA). The DLS analysis was carried out for the more critical evaluation of FCNGL [33]. The DLS evaluation was done at wavelength 264 nm at a temperature of 25 °C.

3.5. Gelation Temperature and Time

Gelation temperature of FCNGL was screened by placing FCNGL formulation in 10 ml vial and placing in a water bath and increasing the temperature slowly from 15 °C to 40 °C at a rate of 0.5 °C min^{-1}. The temperature was maintained stable for 10 min at 15, 25, 37 and 40 °C and finally the vials were inspected for gelation by slanting them at 90° angle and found no longer flow of liquid upon tilting to 90° angle [34]. Gelation time is defined as the time taken by the FCNGL formulation system to completely change from sol to gel at an optimum gelation temperature [35]. The formulation analysis was triplicated and the measurement was repeated as average of triplicated value with SD.

3.6. Entrapment Efficiency (EE)

Entrapment efficiency EE plays crucial role in transporting drugs to the specific site at precise therapeutic dose to attain desired therapeutic efficiency. To measure the EE, the FCNGL formulation was centrifuged at 10000 rpm for 5 min by using digital centrifugation (REMI, NE Delhi, India) to obtain the nanoparticles. The collected supernatant was carefully diluted with PBS of pH 7 and the drug content was determined spectrophotometrically by using UV spectrophotometer (SCHIMADZU, Japan) at 264 nm against a blank solvent [36]. The EE can be calculated by employing the following formula:

$$\%\mathrm{EE} = (\text{weight of drug in FCNGL} / \text{initial weight of drug taken}) \times 100$$

The formulation analysis was triplicated and the measurement was repeated thrice with average value along with SD.

3.7. Rheological Profile

The FCNGL formulation was evaluated for its rheological physiognomies by employing Rheometer (ANTON PAAR) at 25 °C, 30 °C and 35 °C temperature[37]. The formulation examination was triplicated and data was represented with average value along with SD.

3.8. Biodegradation Profile

The biodegradation profile of FCNGL was assessed by exposing the nanogel to three different PBS system of different pH range i.e. acidic (pH 4), neutral (pH 7) and basic (pH 10). Chitosan molecule act as a substrate for lysozyme digestion, therefore the FCNGL was exposed to lysozyme at 37 °C. The nanogel was pelletized by using hydraulic pelletizer and lyophilized. The pelletized nanogel was then immersed in the PBS media with one set having lysozyme and other set is devoid of lysozyme (100 U/ml) and incubated at 37 °C for 45 days [38]. After 45 days of incubation interval the nano-formulations were vacuumed dried for 4–5 h to complete removal of moisture. The degraded amount of weight (Wt) lost by FCNGL was measured by equating with initial weight (Wo) at the starting of study[39]. The degradation amount of FCNGL was calculated by using the formula:

$$\%\ \text{Degradation} = (\mathrm{Wo} - \mathrm{Wt}/\mathrm{Wo}) \times 100$$

The formulation examination was triplicated and data was represented with average value along with SD.

3.9. Swelling Analysis

The swollen FCNGL nano-formulation system displays the degree of swelling. The swelling profile of FCNGL was assessed by engrossing the nanoformulation at different pH range of acidic (pH 4), neutral (pH 7) and basic (pH 10) and measuring the aberration in the physical characteristics of developed FCNGL formulation. The frozen FCNGL was pelletized by using hydraulic pelletizer and exposed to different pH media for about 10–15 min, the FCNGL was then filtered and the final weight was measured (Wf) by equating with initial weight (Wo) of FCNGL[40]. The swelling at each pH was assessed in triplicate and measured by using the formula:

$$\text{Swelling ratio} = (Wf - Wo)/Wo$$

3.10. In-Vitro Drug Release Studies

The *in-vitro* drug release study of 5-FU loaded nanogel was performed by the dialysis bag technique using a shaking incubator (REMI, New Delhi, India) at 100 rpm. Saline phosphate buffer with pH 4, 5, 6 and 7 was employed as dissolution medium to evaluated 5-FU release property from FCNGL in melanoma and healthy melanin environment as melanoma microenvironment exhibits acidic pH with range of 5.56.5 due to the accumulation of lactic acid, whereas the normal melanin pH is around 7.4 [41]. Each dialysis bag (pore size: 12 kD; Sigma Chemical Co., St Louis, MO) was loaded with about 5 ml of FCNGL that was previously separated from un-encapsulated 5-FU by Sephadex G-50 column. The volume and temperature of dissolution medium were 50 ml, and 37±2 °C, respectively. At predetermined time interval 5 ml of sample was withdrawn, replaced with same volume of fresh media, filtered and measured for drug content at 264 nm against blank using UV–Visible spectrophotometer. Mean results from triplicate measurements along with SD were reported [42].

3.11. Ex-Vivo Skin Permeation Studies

For the skin permeation studies, porcine skin was selected for measurement of penetration potential of FCNGL. The penetration potential was evaluated out by using Franz diffusion (FD) cell with a diffusion area of 3.3 cm^2 and volume of 60 ml using porcine tissue [43].

3.11.1. Skin Preparation and Determination of Steady State Flux—The porcine tissue (pig ear) was procured from the local slaughter house. The porcine tissue was sliced into the optimal size by employing surgical scalpel (DISPO VAN, Hindustan syringes and medical devices, Faridabad, India) prior to the deep washing and removal of hair. The tissue was then sandwiched between the donor and the acceptor compartment of FD cell and 1 ml of free drug solution and FCNGL sample was introduced in the donor compartment with phosphate buffer saline (PBS) *pH* 5 was taken in the acceptor compartment as dissolution media and maintained at 37 °C of temperature and continuously stirred at 300 rpm using magnetic stirrer (REMI, India) for 24 h exposure [44]. The test fluids from the acceptor

compartment was intermittently withdrawn and replaced by equal volume of PBS *pH* 5 to maintain the sink conditions. Withdrawn samples were then analyzed by UV spectroscopic method and studies were performed in triplicate [45].

3.11.2. Drug Concentration-Depth Profile—The concentration of drug retained within the porcine tissue was measured by accumulating the skin from the FD cell after 24 h experimental exposure. The collected tissue was cautiously washed with PBS pH 5 and was cut into 50 μm area using cryotome and categorized into 3 sections (upper, middle and lower sections). The retained drug from the skin was then extracted by adding 5 ml ethyl alcohol and continuously stirred for about 10 hours and centrifuged at 5000 rpm for 20 minutes. The supernatant was collected and filtered via 22 mm syringe filter and analyzed for the drug content by UV spectrophotometry technique [46].

3.12. Blood Compatibility Studies

3.12.1. Hemolysis Assay—The hemolysis study was carried out for FCNGL formulation employing fresh human blood. 1.5 ml of ACD (acid citrate dextrose) solution was supplemented to 5 ml of blood sample and incubated for 12 hr at 37 °C (100 μL of blood sample concentration ranging from 0.1 to 1 mg/ml). The incubated samples were centrifuged at 5000 rpm for 5 min to obtain plasma. The obtained plasma was then mixed with 1 μl of 0.01% $NaHCO_3$ solution. The samples were then scanned at 264 nm [47]. The plasma haemoglobin was assessed by employing the following equation:

$$\text{Plasma Hb} = (2\ A\ 264 \times 76.25)$$

The FCNGL concentration was evaluated in triplicate with SD. For the smear slide preparation of FCNGL treated blood sample, “Push and wedge” coverslip technique was used. In this method, a drop of fresh blood was placed on the slide at one end with the help of pipette. The smear was primed by employing spreader slide placed on the blood drop perpendicular at an angle of 45° which spread the blood consistently on the base slide evading any shadowing and patchy width. The smear was the prudently air dried for 30 min for appropriate fixation [48]. The fixed smear was then stained with Leishman’s stain (mixture of polychrome methylene blue and eosin) and waits for about 15 min for cell picking and finally washed with running water and screened under the fluorescent microscope at 100x and 40x objective lens (Olympus, Japan).

Coagulation Assay by Prothrombin Time (PT) and Activated Partial Thromboplastin Time (APTT) Analysis: The PT and APTT analysis assay was employed for determining the coagulation effect of FCNGL nano-formulation. Fresh blood was collected in 10 ml ACD containing tubes and was centrifuged at 5000 for 10 min at 25 °C to obtain platelets poor plasma (PPP). 1000 μl of PPP was mixed with 0.1 μl of sample and incubated at 37 °C for 25 min. After incubation, the PT and APTT were assessed by employing coagulation analyzer reagent kit (CK Prest and Fibriprest, Diagnostica Satgo, France). Mean results from triplicate measurements along with SD were reported [49].

3.13. Cytocompatibilty Studies

3.13.1. Cell Line—Human keratinocyte cell (HaCaT) line was procured from national centre for cell science (NCCS) Pune and was maintained in Dulbecco's modified Eagles Medium (DMEM) supplemented with 10% fetal bovine serum (FBS) and 100 U/mL penicillin, and 100 μg/mL streptomycin (PAA Laboratories GmbH, Austria) antibiotic solution. Cell lines were grown in tissue culture flasks (75 cm2) and maintained at 5% CO2 atmosphere at 37 °C. After attaining the 90% confluency, the cells were trypsinized with 0.25% trypsin EDTA solution (Sigma, USA) [50]. For apoptosis study the HaCaT cells were seeded in 6 well plates (Costars, Corning Inc., NY, USA) at a density of 50,000 cells/well. Furthermore, MTT assay was also employed to determine the viability of HaCaT cell line by seeding 10,000 cells/well in 96 well cell culture plates (Costars, Corning Inc., NY, USA) [50].

3.13.2. MTT Assay—MTT assay was used to evaluate the cell cytotoxicity of FCNGL in HaCaT cell line. The HaCaT cell line was seeded in 96 well plate and incubated with media comprising blank chitosan nanogel, plain 5-Fluorouracil and FCNGL (equivalent concentration of 0.1, 1, 10 and 20 μg/mL, negative control (cells treated with blank media) and positive control (Triton X-100). After optimum incubation time (24 h), the media containing the samples were articulated and cells were washed with HBSS thrice. Subsequently, about 150 μL of MTT solution (500 μg/mL in PBS) was supplemented to each well and re-incubated for 4 h. After 4 h the MTT solution was cautiously articulated and the formazan crystals were then dissolved in 200 μL of DMSO. The optical density (OD) of the resultant solution was then measured at 570 nm using an ELISA plate reader (BioTek, USA) [51].

3.13.3. Apoptosis Assay—The apoptosis assay was carried out to evaluate the cytocompatibilty potential of blank nanogel, plain 5-Fluorourcail and FCNGL on HaCaT cell line. The Annexin V apoptosis analysis is established on the phosphatidyl serine disclosure on the outer layer of the plasma membrane and its interaction with Annexin V. The HaCaT cells were seeded in the 6 well cell culture plate and incubated for overnight at 37 °C and 5 % CO2. The media was extracted and substituted with media containing plain drug, blank nanogel and FCNGL (equivalent to 10 μg/mL) and incubated for 6 h [49]. After the optimum incubation, the media was extracted and the cells were washed with HBSS thrice and treated with Annexin V Cy3.18 (AnnCy3) and 6-carboxyfluorescein diacetate (6-CDFA) (Annexin V Cy3TM Apoptosis Detection kit, Sigma, USA). The HaCaT cells were then analyzed under CLSM under green and red channels for 6-CDFA and AnnCy3, respectively. Additionally, Apoptosis index, i.e., fluorescence intensity ratio of red (measure of apoptosis) and green (measure of viability) channel was also assessed. The fluorescence intensity in the images was evaluated via Image J software (U. S. National Institutes of Health, Bethesda, Maryland, USA) [52].

3.14. Animal Studies

Swiss albino male mice of weight 25–30 g were used for the in-vivo anti-cancer study. Animals were procured from the Veterinary College, Mhow (MP) India. Animals experiments were carried out in Pinnacle Biological Research Institute (PBRI) Bhopal,

India, after due permission of institutional animal ethics committee reference no. PBRI/IAEC/PN42, which is registered with committee for Control and Supervision of Experiments on Animal (CPCSEA), government of India. The mice were maintained under the standard laboratory conditions at 27±2 °C with relative humidity of about 50–70% and at optimum photoperiod (12 h darkness/12 h light cycle) for carrying out in-vivo studies. The mice were normally feed with normal diet chew procured from Hindustan Lever Ltd., Mumbai, India and water was provided ad libitum and bedding was changed twice a week to safeguard the optimum hygienic environments and good comfortable conditions to animals [53].

3.14.1. Skin Irritation Test—The Draize patch test was used on Swiss albino mice to evaluate the irritation potential of the nanogel topical formulations. Male Swiss Albino mice (25–30 g) were housed individually in the animal house with food and water given ad libitum. Mice were divided into four groups (G) (n = 3): G1 – no application (control), G2 – placebo blank chitosan nanogel (no drug), G3 standard 5% w/v 5-FU marketed gel and G4 – FCNGL treated. The back of the mouse was trimmed to remove hair at 24 h prior to the nano-formulation application. The nano-formulation, 1 µl, was applied on the hair-free skin of mice by uniform spreading over an area of 2 cm^2 and skin surface was observed for any visible change such as erythema (redness) after 24, 48 and 72 h of the nanoformulation application [54]. The mean erythema scores were recorded depending on the degree of erythema: no erythema = 0, slight erythema (barely perceptible – light pink) = 1, moderate erythema (dark pink) = 2, moderate to severe erythema (light red) = 3, and severe erythema (extreme redness) = 4.

3.14.2. Experimental Design of DMBA Induced Melanoma Model—DMBA (dimethyl benzene anthracene) is a carcinogen and used for generating chemically induce melanoma in mice model. To induce melanoma with DMBA, a total of 30 male Swiss albino mice were divided into 5 groups consisting of 6 animals in each group (n = 6). Skin carcinogenesis was induced by employing DMBA and croton oil as tumor promoter. Depilatory cream was applied for the elimination of hair from back side (trunk area) of each mouse and the mice were left for 48 h untreated [55]. The mice exhibiting no growth of hair were recruited for the *in-vivo* experimental study.

The 5 groups (G) were subdivided as follows:

G1: Control group with no skin carcinogenesis was induced and received normal saline.

G2: Negative control or toxic control group in which skin carcinogenesis was induced with DMBA (2 µg/2 ml of acetone)

G3: Positive control or Standard group (DMBA + 5% marketed 5 FU gel)

G4: Test group (DMBA + 0.1% w/v FCNGL)

G5: Test group (DMBA + 0.2% w/v FCNGL)

In above procedure, the animals from groups G2 to G5 were received single dose of DMBA (100 μg/100 ml of acetone) over the shaved area of skin. After 2 weeks croton oil (1% v/v in acetone) will be applied as tumor promoter thrice a week till the end of the experiment (16 weeks). The animals of group G3-G5 received the dose of formulations viz., 5% w/v 5-FU marketed gel, 0.1% w/v FCNGL and 0.2% w/v FCNGL topically once a day respectively over the shaven area at concentration of 1μ ml for 16 week. At the end of experiment the mice were euthanized by cervical dislocation method [56].

3.14.3. Biochemical Parameter Estimation—The blood samples were collected from mice in sterilized centrifuged tubes for the biochemical investigation of enzyme levels viz., Catalase (CAT), Superoxide dismutase (SOD), Lipid peroxidase (LP) and Glutathione (GSH) employing ELISA enzyme detection Kit. The collected blood was then centrifuged at 3000 rpm for about 10 min to obtain clear serum [57].

3.14.4. Histological Assessment—The tumor from each mouse was removed after dissection and immediately rinses with normal saline (09% w/v) blotted on Whattman's filter paper, weighed and homogenised with PBS solution (pH 7) and fixed in 10% formalin for 48 h and embedded in paraffin followed by carefully sectioned and microscopically examined by employing haematoxylin and eosin dye to screen the pathological changes by using Fluorescent microscope (Olympus, Japan) under 10x, 45x and 100x objective lens [58].

3.15. Gamma Scintigraphy Evaluation

3.15.1. Preparation of Radiolabelled FCNGL Formulation—The FCNGL was radiolabelled with technetium-99 m (^{99m}Tc) by direct labelling technique. Briefly, about 0.5 ml of FCNGL was mixed with stannous chloride dehydrate solution in the concentration of 100 μg in 100 μl of 0.10 N HCl solutions. The final pH was adjusted to 6.5 by adding 0.5 M $NaHCO_3$ solution [59]. After pH adjustment, sterile 99 m-Tc solution was added to the developed FCNGL with careful and continues mixing followed by incubation for 15–20 min at 37 °C of temperature. The radioactivity of the resultant 99 m-Tc labelled FCNGL before and after incubation was measured carefully. The radiolabelling purity and strength of radiolabelled FCNGL was determined by dialysis bag method [60]. For dialysis about 0.5–1 ml of radiolabelled FCNGL was placed in dialysis bag with pore size 60 kD and dialyzed against 100 ml of normal saline pH 7 at 37 °C for 24 hrs. Aliquots were withdrawn and radioactivity was assessed in triplicate. The radioactivity was evaluated after separating the unlabelled radioactive material. The 99 m-Tc labelled FCNGL was stirred for about 20 min by using digital magnetic stirrer (REMI, New Delhi, India) at 37 °C and then centrifuged. The centrifuged sample was then carefully washed thrice with saline water to eliminate the unlabelled 99 m-Tc traces. The radioactivity present in 99 m-Tc labelled FCNGL was assessed by employing well type gamma scintillation counter (CAPRAC WELL COUNTER, CAPINTEC, CAPRAC-R, UK) [60]. The results of radiolabelling efficiency were measured as the percentage of the total of radioactivity added by using the following formula:

$$\text{Percentage Radiolabelling} = (\text{Post washingcountsinformulation}/\text{Totalcountsadded}) \times 100$$

3.15.2. Bio-distribution & Pharmacokinetic Profile of Radiolabelled FCNGL—

Bio distribution profile is the key element and exists as integral part of any drug delivery system. Bio distribution study profile plays vital role in evaluation of potential and efficiency of drug delivery system by toxicity and safety [61]. For the bio-distribution study, Swiss albino mice weighing 25–30 g were selected as mentioned above in in-vivo protocol. **G2** toxic control group in which skin carcinogenesis was induced with DMBA (2 μg/2 ml of acetone and no treatment of nanogel was performed), **G3**: Standard group (DMBA + 5% marketed 5 FU gel), **G4**: Test group (DMBA + 0.1% FCNGL), **G5**: Test group (DMBA + 0.2% FCNGL) will receive 99 m-Tc FCNGL topically [62]. Each animal from each group were dosed with 200 μl (containing 5% w/v, 0.1 % w/v and 0.2 %w/v of 5-FU in group G3, G4 and G5 respectively). Blood samples were then collected post treatment from the tail vein at 0.5, 1.0, 2.0, 4.0, 8.0 and 12 h of time interval. After the euthanizing the mice other tissues (lung, liver, spleen, kidney and skin) were isolated, washed with PBS at pH 7 and finally weighed. For the entire groups radioactivity present in each tissue /organ was assessed by using shielded well type gamma scintillation counter (CAPRAC WELL COUNTER, CAPINTEC, CAPRAC-R, UK) [63]. Results of radiopharmaceutical uptake/g in tissue were measured and data is represented as percentage of the total amount of radioactivity.

3.15.3. Gamma Scintigraphy Imaging—

For the gamma scintigraphy imaging, Swiss albino mice weighing 25–30 gm were used. The radiolabelled FCNGL nano-formulation loaded with 99 m-Tc was administered topically on the shaven area of 2 cm^2 at the dose of 100–200 μl/mouse consisting 5% v/w, 0.1%w/v and 0.2%w/v of 5-FU of group G3, G4 and G5 respectively. Gamma scintigraphy images were taken by employing single photon emission computerized tomographic camera (LC 75–005, Diacam, Siemens AG, Erlanger, Germany) at 1 h post administration of the radiolabelled samples [64].

3.15.4. Statistical Analysis—

The values were expressed as mean ± SD. The statistical analysis was performed by employing one way ANOVA followed by DUNNET'S T-test. The obtained value will considered statistically significant, if p value is less than 0.01(P value < 0.01) [65].

4. Results and Discussion

4.1. Preparation of 5-Fluorouracil-Chitosan Biodegradable Nanogel (FCNGL)

The 5-FU Chitosan biodegradable nanogel (FCNGL) was engineered by ionic gelation method using sodium TPP as a nontoxic chemical cross-linker. The ionic interaction between the central cationic amino groups extended on the chitosan configuration with active anionic phosphate group of TPP results in significant chemical crosslinking. PF-127 is a hydrophilic copolymer of ethylene oxide and propylene oxide, which form monomolecular micelles at low concentration at 5–10% w/v, whereas it shows multi-molecular aggregates at higher concentration above 15% w/v constituting hydrophobic pendant core encompassing hydrophilic polyoxyethylene backbone exposed to external environment [66]. Micelle development of PF-127 happens above critical micellar concentration in selected solvents system at ambient temperature. Above critical gel concentration (at higher concentration) the

micelles established a lattice structure and form gel. Chitosan-Pluronic 127 nanogel system offers simple synthesis mechanism devoid of any polymerization leading to elevated drug loading efficiency compared to other polymerization nanogel which requires enormous mobilities and comparative less drug encapsulation efficiency also cationic charge on outer chitosan skeleton makes more sensitive nanogel system for the better ion attraction mechanism between positive charge nanogel and negative charge cancerous cell membrane [67].

4.2. Particle Size, Zeta Potential and Transmission Electron Microscopy

The success of topical chemotherapy of melanoma is largely dependent of nano-sized particle size of gel. The smaller particle size ranging 100–400 nm can penetrate deep into dermis layer by endocytosis mechanism which enables the nano-sized molecules to penetrate the tissue and enhance drug delivery efficacy at tumor angiogenic blood vessel [68]. Towards this end, we used transmission electron microscopy (TEM) of FCNGL nanogels which revealed spherical shape and nanosized particle distribution (Fig. 1a & b). To understand surface pattern of nanogel, we visualized them in SEM and it showed nice and smooth three-dimensional spherical particles (Fig. 1c & d). Both TEM and SEM data indicates nanosize range of FCNGL particles with size range of 100–180 nm, exhibiting consistent and nanosized range particle distribution. The particle size histogram of TEM analysis clearly demonstrates that majority of the nanoparticles falls in the range of 100–200 nm which reflects the optimum size favouring topical delivery at melanoma site. The Zeta potential of FCNGL formulation was found to be + 43.15 m. The cationic charge is a favourable feature for enhancing cell uptake and stability of nanoparticles. The existence of -OH and -NH_2 group in chitosan is the vital elements for the pH responsive 5-FU release from FCNGL in acidic tumor microenvironment. The key factor of FCNGL nanoformulation is the pH responsive nature, which govern as driving force in the efficient topical/transdermal delivery. The pH of the developed FCNGL was found to be 6.1 when evaluated by digital pH meter (Shimadzu, Japan) which significantly mimic the pH environment of melanoma and exhibited a suitable topical carrier system feature against melanoma

4.3. Scanning Electron Microscopy

The outcomes of SEM analysis shows very distinct morphology of particles due to severe aggregation of nanoparticles (hydrophilic chitosan polymer amiable to accommodate moisture) (Fig. 1d) during lyophilization process which affect the evaluation of exact particle size of developed nanoparticles, exhibiting larger particle size compared to TEM analysis, despite aggregation, Fig. 1c indicates that the size range is between 100–250 nm which is suitable for topical delivery, validated by the SEM histogram. These features are indicative of efficient topical/transdermal delivery with enhanced skin penetration. The minor assemblage of particles as showed in TEM is indicating the hydrophilic nature of FCNGL nano-system that makes cordial association of chitosan component to form nanogel.

4.4. Dynamic Light Scattering (DLS)

The dynamic light scattering (DLS) profile demonstrates advanced and more distinct analysis of size, distribution pattern and their dispersity in the solution phase. The DLS pattern (Fig. S3 a & b) indicates that size of FCNGL particles are in range of 120–180 nm,

with narrow polydispersity index (0.213), which favours the skin layer penetration as a potent topical chemotherapeutic delivery. The acquired features of nano-size FCNGL plays a key role in effective delivery of 5-FU to melanoma through EPR effect [69].

4.5. Gelation Time Analysis

Gelation time denotes the time tangled by the FCNGL nano-system to completely transform from sol to gel at ambient temperature. The gelling time of FCNGL was about 49 sec. at 28–30 °C of temperature, which indicates significantly faster gelation property of FCNGL in presence of 22% of PF-127 polymer and this gel reverses back to sol phase immediately at 8 °C. As the concentration of PF-127 increased the gelling time and viscosity of FCNGL was also increased significantly, so optimization of FCNGL plays crucial role for optimum nanogel characteristics to comply with dermal environment. This gelation property of FCNGL supports the controlled release property of 5-FU from nanogel in deep epithelial tissue embedded melanoma environment.

4.6. Rheological Profile

The FCNGL showed distinct rheological profile, and the viscosity of FCNGL system is of about 3122 cps. The rheological feature of FCNGL is varied with temperature and it has been found FCNGL diverse rheological pattern at 25 °C but found to be constant at 30 °C. The variability of rheological property is possible due to encapsulation of 5-FU in FCNGL. The rheological profile study indicates, as the temperature increases from 25 °C to 30 °C there is a peripheral amount of increment in viscosity with increase in shear rate.

4.7. Swelling Analysis

Swelling study of FCNGL was performed in range of pH 4, 7, and 10 to understand the stability of nanogel architecture. The data from Fig. S4 indicates swelling tendency of FCNGL in acidic condition (pH 4) is higher, whereas at neutral condition (pH 7) it is decreased. The significant increase of swelling capacity of FCNGL at acidic pH is possibly due to protonation of -OH and $–NHCOCH_3$ group in chitosan nanoparticles, resulting enhanced ionic attraction and water absorption. This data demonstrate that FCNGL will be function as tumor pH responsive 5-FU delivery agent for targeted tropical chemotherapy, while healthy tissue remained unaffected.

4.8. Entrapment Efficiency

Entrapment efficiency (EE) of 5-FU to FCNGL was revealed about 55%, which is suitable in achieving desired drug dosing for in vivo. The drug concentration and the time of incubation plays key role in the EE. Elevated incubation time and optimum drug concentration, results in good EE. The EE displayed by the FCNGL nanoformulation is due to the high leaching out of drug from the nanogel matrix due to the hydrophilic nature of FCNGL. Erstwhile to the concentration of drug and incubation time the stirring speed and stirring time along with sonication interval also play vital role in the EE, high rate of stirring for the longer period of time may results in early eruption of FCNGL particles which leads to the leaching out of drug from its compartment. Also longer interval sonication exposure at higher amplitude can

also cause the early burst out of drug due to elevated swelling befalls into the surrounding aqueous environment.

4.9. Biodegradation Assessment

Biodegradation assessment provides crucial information about tumor cell specific drug release property and biocompatible nature of nanogel. The effective delivery of nanoparticle in tumor cells depends on the endocytosis, followed by lysosomal degradation to release the drug in cytosol. Biodegradation profile (Fig. 2) FCNGL at variable pH showed 85–90% of FCNGL degradation in the presence of lysosomal enzyme and about 55–60% in the absence of lysozyme enzyme, demonstrating effective degradation of FCNGL in lysosome mimetic condition. Potent degradation capacity of FCNGL is possibly due to lysosomal proteases, such as cathepsin-b mediated degradation of amide bond that present in chitosan[25]. This data supports the ability of FCNGL for efficient delivery of 5-FU to melanoma cells.

4.10. In-vitro Drug Release Studies

The In vitro drug release profile of FCNGL was carried by employing dialysis bag method in phosphate buffer saline solution (PBS) at pH 4.0, 5.0, 6.0 and 7.0 at 37 °C. The drug release behaviour of FCNGL nanoformulation at diverse pH was demonstrated in Fig. S5. The configuration documented from the FCNGL at different pH range displayed the biphasic behaviour with initial burst in early 1–5 hours followed by slow release. The 5-FU release from the nanogel matrix is directed by the diffusion mechanism which is completely dependent on the degree of de-acetylation and molecular weight of chitosan molecule. The early burst of the nanogel particles is due to the hydrophilic nature of chitosan molecules, which have greater tendency to lodge large amount of water or aqueous molecules leads to the early degradation of nanogel particles through hydrolysis. The degradation or erosion phenomenon depicted by FCNGL is symbiotically depends on the ionic interaction and degree of de-acetylation of chitosan. Higher the degree of de-acetylation meagre is the degradation or erosion. The developed biodegradable FCNGL exhibits 75% degree of de-acetylation of chitosan strength, portraying the biphasic release pattern revealing initial bursting of nanogel particles followed by slow and sustained release. The inclusive cumulative release of 5-FU varied from 35% to 70% in 48 hours. The optimized FCNGL nanoformulation showed early release of about 30–45% at pH 7 in 24 hours, due to the slight alteration in pH and aggregation of nanoparticles because of having tendency of absorbing water molecules which unintentionally degrade the chitosan core and enables slight drug release. Eventually the drug release at pH 7 is very slight and delayed over the course of 24–48 hours compare to pH 5 and indicating non-viability towards the normal melanin cells. The transitional pattern of FCNGL was documented of about 50–60% at pH 4 exhibiting the extreme release of early acid activation by the nanoformulation and mimicking the skin physiology. The supreme release pattern was recorded at pH 6 & 5 of nearly about 70–85 % unveiling the pH responsive behaviour by sustained release pattern of FCNGL formulation in 24–48 hours duration. At both pH 6.0 and 5.0 the FCNGL discovered initial burst due to hydrophilic nature of the outer chitosan layer and rapid swelling mechanism, but after 3 hour the FCNGL exhibit slow and constant release n following the Higuchi model. The cumulative drug release of the optimized FCNGL formulation followed the Higuchi’s kinetics model displaying sustained release behaviour

due to hydrophilic cationic chitosan particles and revealing the pH sensitive behaviour and site specific drug release physiognomies mimicking melanoma conditions.

4.11. Ex-vivo Studies

4.11.1. Steady State Flux—The penetration potential data obtained from the UV spectrophotometric analysis revealed the significant permeation of FCNGL over free drug solution. The cationic chitosan nanogel showed enhanced penetration efficiency over free drug solution due to better muco-adhesion over skin facilitation sustained release of 5–FU at targeted area. The Ex-vivo data clearly depicted out that the FCNGL showed about 80–85% of 5-FU released (Fig. 3 a) from the nanogel core exhibiting noteworthy permeation rate in 24 h compared to the meager release of 40–45% of free drug solution due to early adsorption over skin area. The flux ratio portrayed by FCNGL in 24 h release study exhibited greater penetration potential when analyzed by Student's t test. The governing mechanism behind the FCNGL permeation is that the nanoformulation permeates transcellularly i.e., through hair follicle pathway or by intracellularly i.e., via sweat glands pathway. The above penetration studies profile showed the significant and remarkable ex-vivo penetration efficiency of FCNGL in 24 h release study compared to lesser penetration of free drug solution by virtue of steady state flux. The chitosan nanogel has a tendency to interact with the anionic lipids and keratin due to cationic outer core charge exhibited by the chitosan skeleton. But in the free drug solution due to more hydrophilicity and surface adsorption meager penetration occurred.

4.11.2. Concentration Depth Estimation—The drug concentration depth profile data obtained by the 24 h experimental exposure of porcine tissue depicted enhanced retention of FCNGL in the skin layers. The concentration depth data validated the images of tissue regarding retention and permeation of FCNGL system showing noteworthy penetration at each epidermis layer (upper, middle and lower layer) (Fig. 3 b). The results obtained from concentration depth profile confirmed that the penetration potential and retention of FCNGL is significant (analyzed by Student t-test) and noteworthy in 24 h exposure exhibiting greater retention at upper epidermis layer, middle epidermis and lower epidermis layer compared to middle and lower layer meager retention exhibited by free drug solution. The pH responsive and cationic nature of chitosan nanogel (FCNGL) enabled the ionic interaction with skin lipids proves its efficient delivery of versatile bioactives against many diseases like skin cancer, skin eczema etc. Therefore it can be forthrightly demonstrated out that cationic chitosan nanogel system offers great therapeutic benefits on topical delivery against skin cancer.

4.12. Blood Compatibility Studies

4.12.1. Hemolysis Study—In the clinical platform the *in vitro* infusion of 5-FU to patients showed changes in their erythrocyte's morphology, membrane fluidity and ionic balance. This reduces the oxygen transportation capability of red blood cells (RBCs) resulting in insufficient supply of blood to the heart leading to cardiotoxicity [24]. We hypothesized to develop sustain drug release topical FCNGL nanogel that can protect the direct exposer of 5-FU to blood circulation and effectively deliver the drug load to the melanoma environment. The blood compatibility effect of FCNGL at varied concentration

displayed a remarkable decrease in hemolysis effects as depicted in Fig. 4a & b, when compared with positive control. It is significantly evaluated out that hemolysis effect exist only in positive control vial, while no lysis of RBCs were observed in negative control or in formulation vials (Fig. 4b). The clear plasma at concentration 0.2–0.8 shown in Fig. 4b revelas no lysis of RBCs compared to the positive control which shows opaque red color plasma indicating the lysis of RBCs and leach out of heam and other contents. In the range of 0.2–0.6 mg/ml concentration of FCNGL there is negligible hemolysis of RBCs were seen while nominal increment of hemolysis was found with increasing concentration of FCNGL to 0.8 and 1.0 mg/ml and above. The hemolytic ratio of FCNGL is showing less than 4 %. This is considered as safe in clinic as per ISO/TR 7406 ethical course of action, which allows maximum 5 % hemolysis, suggesting the FCNGL nanogel meets fundamental clinical safety requirement. Further to evaluate hemolytic effect of FCNGL on erythrocyte's morphology, we visualized blood samples under light microscope with Leishman's reagent staining or bright field images (Fig. 4 c-h). Fig. 4 c, positive control group indicates coagulation and lysis of RBCs, whereas no significant coagulation and rapture of RBCs were observed in all concentration of FCNGL treated blood (Fig. 4 d-h). The hemolysis outcomes confirm that FCNGL nanogel shows low toxicity to erythrocytes lysis and it is competent for melanoma therapy purpose. The hemolysis results efficiently validated the permeation studies and peneteration potention of FCNGL on topical application as the minor nanoformulation reaches to the blood circulation after exhibiting its potency in targered and desired site on longer exposure and retention. The hemolytic ratio justified the biological safe margin of syntheiszed FCNGL and efficiently validated by ex-vivo permeation study that on topical application the formulation (minor traces) also reaches to the blood circulation.

4.12.2. PT & APTT Assay—PT or APTT analyses were performed to understand the biocompatibility potential of FCNGL. The PT assessment indicates the extrinsic pathway and APTT reveals the intrinsic pathway of blood coagulation phenomenon[17]. The coagulation time of PT and APTT for FCNGL treatment is 12.9 Sec. and 31 Sec. respectively (Fig. S6 a), and there is no significant coagulation is observed for FCNGL treated PT and APTT blood tube (Fig. S6 b). Both the data indicate safety margin of newly developed 5-FU nanogel.

4.13. Cytocompatibilty Assay

4.13.1. MTT Assay—The MTT cytotoxicity result demonstrates that plain 5-fluorouracil, blank nanogel and FCNGL are cytocompatible at all concentration (Fig. 5a). The cytotoxicity result showed that the FCNGL nanoformulation is slightly more toxic to HaCaT cell compare to plain 5-FU exhibiting enhanced cell cytotoxicity effect of FCNGL by HaCaT cell and found statistically significant when analysed by student's T test. The developed FCNGL and plain 5-FU shows noteworthy cell toxicity towards the cancer cell when evaluated in HaCaT cell lines due to the free radical scavenger property of 5-FU which exhibit selective toxicity towards cancer cell rather than normal cell. The blank nanogel showed negligible toxicity and showed identical effect when compared with media as it devoid of any anticancer drug or property. The combination biodegradable chitosan and anticancerous 5-FU diminishes the toxic effect on normal HaCaT cell. The MTT assay also

established that the FCNGL conserved the potential and strength of the 5-FU towards cancer cell avoiding toxicity to the normal proposing FCNGL as impeccable topical nanocarrier against melanoma with negligible toxicity towards normal cells.

4.13.2. Apoptosis Assay—The outcomes of apoptosis demonstrates that both FCNGL and plain 5-Fluorouracil exhibit competent apoptosis potential at higher concentration compared to blank nanogel which shows negligible apoptosis (Fig. 5b). The antimetabolite 5-Fluorouracil exhibit inborn apoptosis effect by varied phenomenon. The 5-FU exhibit both intrinsic (mitochondrial) and extrinsic (death receptor) apoptosis effect. The main reason behind innate apoptosis is that 5-FU induces apoptosis by acting in the G2 phase and thus shows mitochondrial apoptosis mechanism. In the extrinsic apoptosis pathway phase, 5-FU acts as death activator by provoking cell surface receptor. Initiating the cell surface receptor, activation of caspase-8 and initiation of caspase cascade take place by 5-FU. The cationic charge of FCNGL also enable noteworthy apoptosis by permitting the entry of nanoparticles via stratum corneum or hair follicle pathways through endocytosis and interacts to the negatively charge cancer (melanoma) cell. The charge interaction or ionic attachment enables efficient degradation of chitosan core results in onsite release of antimetabolite at targeted site without counteracting the normal cells exhibiting biosafety and cytocompatibilty of FCNGL nanogel system.

4.14. In-Vivo Animal Studies

4.14.1. Tumor Growth and Tumor Diameter Profile—Tumor growth inhibition effect of FCNGL was evaluated in DMBA induced melanoma model. The Fig. 6a indicates the treatment received and tumors growth by the mice in sixteen week study except group G1 (received only saline) while Fig. 6b indicates the tumor burden and percent of tumor incidence in the mice of different treatment groups in 16 week studies. Mice of G2 exhibit multiple tumor nodule formation, 90% mortality rate and it was considered as 100% tumor growth. Group G3 (5% w/v 5-FU gel) revealed 61% of tumor incidence rate and about 49% mortality rate with prominent tumor inhibition potency. Whereas, group G4 (0.1% w/v 5-FU nanogel) exhibits significant regression in tumor formation with 46% tumor incidence rate and less than 50% mortality rate (35 %) compared to G3. Treatment group G5 (0.2% w/v 5-FU nanogel) shows significant tumor inhibition profile revealing only few numbers of tiny sized melanoma nodules with 33% tumor incidence with minimum moratlity rate of about 21% which is remarkable compared to normal and toxicant group. The tumor growth suppression profile demonstrates the apex potential of FCNGL against the highly aggressive melanoma and the prominent anti-tumor effect of FCNGL, even in 50% lesser doses of clinically used 5-FU formulation. The profound anti-cancer effect of FCNGL reflects the nanosize particles of developed nanogel which accumulate in the tumor site through EPR effect, exhibits sustain release of 5-FU with cationic nature of the nanogel that led to faster uptake in tumor cells. Anti-tumor activity of FCNGL opens a new window of topical chemotherapy for the highly aggressive melanoma with reduced side effect and dose frequency (once a day application) which is novel and par effective in current scenario compared to other topical 5-Fluorouracil gel (Efudex) aginst skin cancer especially SCC (Squammous cell carcinoma) and BCC (Basal cell carcinoma) [70]. Along with the anti-cancer effect, the skin irritation symptoms of FCNGL were also lacking any significant sign

of irritation and no edema formation was observed in FCNGL treatment, which indicated its safety and acceptability for topical FCNGL administration. Fig. 6c and 6d reveals the tumor diameter (millimetre scale) pictograph profile on 8wks, 12wks, and 16wks post-treatment of different treatment groups, 5-FU nanogel treatment groups (G4 & G5) reveals significant decline in tumors size and appears smaller in diameter compared to the standard group of 5% w/v 5-FU marketed gel and negative control group (G2). The diameter differs greatly in G4 and G5 when analysed and compared with G2 and G3 statistically (student's T-test) which reveals enhanced anticancer potential of developed 5-FU nanogel system when administered once a day. Thus, order anti-cancer potency is followed to be G5 > G4 > G3 > G2 based on tumor diameter. This chitosan nanogel system exhibits significant reduction in tumor diameter size in different week treatment along with reduction in dose frequency as it requires once a day application due to sustained release action compared to conventional gel which required twice or thrice application in a day. The chitosan here plays vital role in synthesis of sustained released biodegradable nanaogel system (FCNGL) with mucoadhesive property leading to enhanced physiochemical stability, pharmacological potential and negligible local toxicity compared to other synthetic polymer [71] or modified chitosan gel system [72].

4.14.2. In-Vivo Biochemical Parameter Analysis—Biochemical parameters such as, CAT, GTH, LP and SOD were evaluated in blood of different treatment groups. From the biochemical parameter profile (Fig. 7), G2 treatment shows marked deviations in all the enzyme level since it does not receive any kind of treatment and were amiable for DMBA only. The noticeable decline level of GTH, CAT and SOD and enhance level of LP for G2 mice is due to the continuous exposure of carcinogen (DMBA) and inflammatory agent (croton oil). G3 mice showed little decline of the LP level, significant enhancement in the GTH, CAT and SOD level as compare to the G2 treatment. Analysing the G4 and G5 treated mice, which exhibit significant elevation of all three GTH, CAT and SOD enzymes level and decline in the LP level when compared to the G2 mice and marketed 5-FU formulation. Thus, FCNGL treatment led to enhance the anti-oxidant and detoxifying level in blood that is linked with tumor growth inhibition and it suggests that our 5-FU nanogel is compatible for transdermal melanoma therapy.

4.14.3. Histology Profile—The histology profile of melanoma affected skin in nanogel treated and control mice was performed at the end of the experiment and skin tissue sections were analysed under light microscope to understand the recovery of skin layer due to treatment regimen. Fig. 8 depicted that the G2 mice have significant disruption in the squamous layer of skin with keratin blow out. In G3 and G4 there is healthy regeneration of dermis layer, healing of keratinized squamous layer than the control G2 mice skin. When analysing G5 treated mice melanoma affected skin, it shows significant revival of dermis layer along with proper distribution of keratinized squamous tissue than compared G2 control and G3 treated mice skin histology profile. This histology study ensures the better uptake and distribution of FCNGL in melanoma affected area that directly linked with anti-cancer efficacy and tumor targetability of FCNGL. This data supports the 5-FU loaded chitosan nanogel as an alternative topical nano-chemotherapeutic for targeted drug delivery of melanoma.

4.15. Gamma Scintigraphy Analyses

4.15.1. Radiolabelling Analysis—To understand the localization potential of nanogels in melanoma nodules, we radiolabelled FCNGL and control formulation with 99 m-Tc. The radiolabelled nano-formulations were applied to melanoma bearing mice and whole-body imaging was performed after 60 min post treatment by non-invasive gamma scintigraphy particle imager. The gamma scintigraphy images (Fig. 9) demonstrates that the 99 m-Tc labelled FCNGL of both G4 and G5 treated mice is significantly accumulated in the dermal region (hind leg portion). Whereas for G3 treatment 99 m-Tc is majorly accumulated in tumor with larger area that possibly due to accumulation in spleen. In G2 treatment, the accumulation of 99 m-Tc occurs in tumor nodules as well as in liver that indicates the non-specificity of free 99 m-Tc. That's why it is important to synthesize nanogel formulation (FCNGL) for achieving tumor specific delivery with reduced non-specific liver, spleen uptake.

4.15.2. Bio-distribution& Pharmacokinetic Profile—The pharmacokinetic pattern of radiolabelled FCNGL with the dose of 5% (standard marketed gel) (G3), 0.1% w/v (G4) and 0.2% w/v (G5) of 5-FU topical nanogel was measured after single treatment on healthy Swiss albino mice. The pharmacokinetic parameters of 99 m-Tc labelled nano-formulation were recorded in blood and skin (Table 1). For G4 and G5 treatment the concentration, the maximum (C_{max}) values of skin were slightly enhanced and significantly increased of AUC intensity than the 5% marketed formulation (G3). The T_{max} and AUC values of G4 and G5 treated blood samples were found elevated compared to G3 treated mice. The skin and blood pharmacokinetics data indicates that FCNGL has sustained drug releasing characteristics and deep tissue penetration potential reflects the affirmative parameter for topical chemotherapy. The bio-distribution of 99 m-Tc labelled FCNGL in different tissues of healthy mice were evaluated at different time intervals after post treatment such as, 0.5, 1, 2, 4, 8 and 12. Fig. S7 shows the significant amount of 99 m-Tc even after 6 h of post treatment and insignificant accumulation of 99 m-Tc in healthy organs, spleen, liver and kidneys. Thus the site specific delivery potential (SSDP) results obtained from radiolabelled FCNGL indicate enhanced transportation of cytotoxic drug to the targeted site upon topical administration.

5. Conclusions

In this study, we engineered a 5-FU loaded nanogel based topical delivery strategy for effective therapy of melanoma. The so engineered FCNGL nanogel exhibited pH responsive sustain 5-FU release, and demonstrated significant therapeutic potential even at very low drug doses (0.2% 5-FU w/v) compared to the marketed product. The FCNGL displayed nanosized particle size distribution, biodegradable property in lysosomal enzyme mimetic condition, suggesting its compatibility for intracellular drug delivery. The FCNGL has negligible blood hemolysis property, that is considered as a safe medication for in vivo drug delivery. The anticancer effect of topically used low dose FCNGL (0.2% 5-FU w/v) is significantly higher compared to the marketed high 5-FU dosed formulation (5% 5-FU w/v), against chemically induced melanoma animal tumor model. The tumor growth inhibitory effect of FCNGL is associated with high accumulation of 5-FU in skin layer causing

regeneration of keratinised squamous skin layer, providing positive modulation of antioxidant enzymes resulting in reduction of drug associated toxic effects. Whole body Gamma scintigraphy images of mice with treatment of 99 m-Tc labelled FCNGL corroborated the efficacy and selective tumor accumulation of FCNGL with low spleen and liver uptake. Overall the new approach of developing biocompatible, pH responsive, nanosized gel opens a novel avenue for topical melanoma therapy and reduces undesirable side effect to healthy tissues and cells warranting further investigations.

Supplementary Material

Refer to Web version on PubMed Central for supplementary material.

Acknowledgement

The research work was supported by Indian Council of Medical Research, New Delhi, India with a Senior Research Fellowship to Prashant Sahu, Ref No.45/28/2014-Nan/BMS dated 21/03/2016. Authors wish to thank Adina Institute of Pharmaceutical Sciences, Sagar (MP), India and Pinnacle Biological Research Institute (PBRI) Bhopal, India for providing the Institutional Animal Ethical Committee permission to undertake animal experimentation work. Thanks are also due to V-Scan Laboratory, Bengaluru, India for Gamma Scintigraphy work. We pay our acknowledgement to Sophisticated Instrumentation Analysis Laboratory, Dr. Harisingh Gour Central University, Sagar, M.P. India for TEM, SEM and other facilities. We thank SRL laboratory, Gurgaon, India for Hemolysis, PT & APTT studies as well as for providing the histology facilities. We are thankful to Centre for Pharmaceutical Nanotechnology, Department of Pharmaceutics, National Institute of Pharmaceutical Education and Research (NIPER), Mohali Punjab, India for pharmacokinetic assessment work. Sushil K. Kashaw wish to acknowledge the University Grants Commission, New Delhi for the award of Raman Postdoctoral Research Fellowship in Use-inspired Biomaterials & integrated Nano Delivery (U-BiND) Systems Laboratory, Department of Pharmaceutical Sciences, Eugene Applebaum College of Pharmacy and Health Sciences, Wayne State University, Detroit, MI, USA.

References

[1]. Jing X, Michael CW, Theoharis CG, The use of immunocytochemical study in the cytologic diagnosis of melanoma: evaluation of three antibodies, Diagn Cytopathol. 41 (2013) 126–130. [PubMed: 22021247]

[2]. Wang D, Lippard SJ, Cellular Processing of Platinum Anticancer Drugs, Nat. Rev. Drug Discov 4 (2005) 307–320. [PubMed: 15789122]

[3]. Orchard G, Comparison of immunohistochemical labelling of melanocyte differentiation antibodies melan-A, tyrosinase and HMB 45 with NKIC3 and S100 protein in the evaluation of benign naevi and malignant melanoma, Histochem J. 32 (2000) 475–481. [PubMed: 11095072]

[4]. Theos AC, Truschel ST, Raposo G, Marks MS, The Silver locus product Pmel17/gp100/Silv/Me20: controversial in name and in function, Pigment Cell Res. 18 (2005) 322–336. [PubMed: 16162173]

[5]. Gajjar NA, Cochran AJ, Binder S, Is MAGe-1 expression in metastatic malignant melanomas really helpful? Am J. Surg. Pathol 28 (2004) 883–888. [PubMed: 15223957]

[6]. Zalla MJ, Lim KK, Dicaudo DJ, Gagnot MM, Mohs micrographic excision of melanoma using immunostains, Dermatol. Surg 26 (2000) 771–784. [PubMed: 10940065]

[7]. El Shabrawi-Caelen L, Kerl H, Cerroni L, Melanin-A: not a helpful marker in distinction between melanoma in situ on sun-damaged skin and pigmented actinic keratosis, Am. J. Dermatopathol 26 (2004) 364–366 33. [PubMed: 15365366]

[8]. Beltraminelli H, Shabrawi-Caelen L, Kerl H, Cerroni L, Melan-apositive “pseu-domelanocytic nests”: a pitfall in the histopathologic and immunohistochemical diagnosis of pigmented lesions on sun-damaged skin, Am. J. Dermatopathol 31 (2009) 305–308. [PubMed: 19384076]

[9]. Oh J, Drumright KR, Siegwart DJ, Matyjaszewski K, The Development of Microgels/Nanogels for Drug Delivery Applications, Prog. Polym. Sci 33 (2008) 448–477.

[10]. Sahu P, Das D, Mishra VK, Kashaw V, Kashaw SK, Nanoemulsion: A Novel Eon in Cancer Chemotherapy, Mini Rev, Med. Chem 2 (2017) 1–22.

[11]. Chacko RT, Ventura J, Zhuang J, Thayumanavan S, Polymer Nanogels: A Versatile Nanoscopic Drug Delivery Platform, Adv. Drug Deliver. Rev 64 (2012) 836–851.

[12]. Alsaab HO, Sau S, Alzhrani R, Tatiparti K, Bhise K, Kashaw SK, Iyer AK, PD-1 and PD-L1 checkpoint signaling inhibition of cancer Immunotherapy: Mechanism, Combinations, and clinical outcome, Front. Pharmcol 8 (2017) 561–574.

[13]. Das D, Sahu P, Mishra VK, Kashaw SK, Nanoemulsion-the Emerging Contrivance in the Field of Nanotechnology, Nanosci. Nanotech. Asia 2 (2017) 1–22.

[14]. Kabanov AV, Vinogradov SV, Nanogels as Pharmaceutical Carriers: Finite Networks of Infinite Capabilities, Angew. Chem., Int. Edit 48 (2009) 5418–5429.

15. Sahu P, Kashaw SK, Sau S, Iyer AK, Stumuli-Responsive Bio-Hybrid Nanogels: an Emerging Platform in Medicinal Arena, Global J. Nanomed 1 (2017) 1–3.

[16]. Vishwakarma APS, Vishwe A, Sahu P, Chaurasia A, Magical Remedies of Terminalia arjuna Roxb, Int. J.Pharma. Archive 2 (2013) 189–201.

[17]. Du JZ, Sun TM, Song WJ, Wu J, Wang J, A Tumor-Acidity-Activated Charge Conversional Nanogel as an Intelligent Vehicle for Promoted Tumoral-Cell Uptake and Drug Delivery, Angew. Chem., Int. Edit 49 (2010) 3621–3626.

[18]. Das D, Sahu P, Kashaw V, Kashaw SK, Formulation and Assessment of In Vivo Anti-Inflammatory Potential of Omega-3-Fatty Acid Loaded Self Emulsifying Nanoemulsion, Curr. Nanomed 7 (2017) 47–58.

[19]. Smith KJ, Germain M, Skelton HG, Squamous cell carcinoma in situ Bowen's disease in renal transplant patients treated with 5% imiquimod and 5% 5-fluorouracil therapy, Dermatol Surg. 27 (2001) 5611–5614.

[20]. Epstein E, Does intermittent "pulse" topical 5-fluorouracil therapy allow destruction of actinic keratoses without significant inflammation? J. Acad. Dermatol 38 (1998) 77–80.

[21]. Pearlman DL, Weekly pulse dosing: effective and comfortable topical 5-fluorouracil treatment of multiple facial actinic keratosis, J. Am. Acad. Dermatol 25 (1998) 665–667.

[22]. Marrero GM, Katz BE, The new fluor-hydroxy peel. A combination of 5-fluorouracil and glycolic acid, Dermatol. Surg 24 (1998) 973–978. [PubMed: 9754085]

[23]. Loven K, Stein L, Furst K, Levy S, Evaluation of the efficacy and tolerability of 0.5% fluorouracil cream and 5% fluorouracil cream applied to each side of the face in patients with actinic keratosis, Clin. Ther 24 (2002) 990–1000. [PubMed: 12117087]

[24]. She W, Luo K, Zhang C, Wang G, Geng Y, Li L, He B, Gu Z, The Potential of Self-Assembled, pH-Responsive Nanoparticles of MPEGylated Peptide Dendron-Doxorubicin Conjugates for Cancer Therapy, Biomaterials. 34 (2013) 1613–1623. [PubMed: 23195490]

[25]. Kannadorai RK, Chiew GGY, Luo KQ, Liu Q, Dual functions of gold nanorods as photothermal agent and autofluorescence enhancer to track cell death during plasmonic photothermal therapy, Cancer Lett. 357 (2015) 152–159. [PubMed: 25444933]

[26]. Gao Y, Li Y, Wang Y, Chen Y, Gu J, Zhao W, Ding J, Shi J, Controlled synthesis of multilayered gold nanoshells for enhanced photothermal therapy and SERS detection, Small 11 (2015) 77–83. [PubMed: 25223387]

[27]. Kang S, Bhang SH, Hwang S, Yoon JK, Song J, Jang HK, Kim S, Kim BS, Mesenchymal stem cells aggregate and deliver gold nanoparticles to tumors for photothermal therapy, ACS Nano 10 (2015) 9678–9690.

[28]. Yang X, Yang M, Pang B, Vara M, Xia Y, Gold nanomaterials at work in biomedicine, Chem. Rev 115 (2015) 10410–10488.

[29]. Aioub M, Elsayed MA, A real-time surface enhanced raman spectroscopy study of plasmonic photothermal cell death using targeted gold nanoparticles, J. Am. Chem. Soc 138 (138) (2016) 1258–1264. [PubMed: 26746480]

[30]. Shanmugam V, Selvakumar S, Yeh C, Near-infrared light-responsive nanomaterials in cancer therapeutics, Chem. Soc. Rev 43 (2014) 6254–6628. [PubMed: 24811160]

[31]. Chen W, Yuan Y, Cheng D, Chen J, Wang L, Shuai X, Co-delivery of Doxorubicin and siRNA with reduction and pH dually sensitive nanocarrier for synergistic cancer therapy, Small. 10 (2014) 2678–2687. [PubMed: 24668891]

[32]. Chaurasia A, Sahu P, Gajbhiye V, Improved anticancerous activity of Indian aloe loaded chitosan microspheres, Int. J. Pharm. Arch 3 (2013) 71–76.

[33]. Sahu P, Kashaw SK, Kushwah V, Sau S, Jain S, Iyer AK, pH responsive biodegradable nanogels for sustained release of bleomycin, Bioorg. Med. Chem 25 (2017) 4595–4613. [PubMed: 28734664]

[34]. Sahu P, Kashaw SK, Jain S, Sau S, Iyer AK, Assessment of penetration potential of pH responsive double walled biodegradable nanogels coated with eucalyptus oil for the controlled delivery of 5-fluorouracil: In vitro and ex vivo studies, J Controlled Rel. 253 (2017) 122–136.

[35]. Cheng R, Meng F, Deng C, Klok HA, Zhong Z, Dual and multi-stimuli responsive polymeric nanoparticles for programmed site-specific drug delivery, Biomat. 14 (2013) 3647–3657.

[36]. Wang W, Cheng D, Gong F, Miao X, Shuai X, Design of multifunctional micelle for tumor-targeted intracellular drug release and fluorescent imaging, Adv. Mater 24 (2012) 115–120. [PubMed: 22143956]

[37]. Cabral H, Matsumoto Y, Mizuno K, Chen Q, Murakami M, Kimura MK, Terada Y, Kano MR, Miyazono K, Uesaka M, Accumulation of sub-100 nm polymeric micelles in poorly permeable tumours depends on size, Nat. Nanotechnol 6 (2011) 815–823. [PubMed: 22020122]

[38]. Perrault SD, Walkey C, Jennings T, Fischer HC, Chan WCW, Mediating tumor targeting efficiency of nanoparticles through design, Nano Lett. 9 (2009) 1909–1915. [PubMed: 19344179]

[39]. Huo S, Ma H, Huang K, Liu J, Wei T, Jin S, Zhang J, He S, Liang X, Superior penetration and retention behavior of 50 nm gold nanoparticles in tumors, Cancer Res. 73 (2013) 319–330. [PubMed: 23074284]

[40]. Ukmar T, Maver U, Planinšek O, Kaučič V, Gaberšček M, Godec A, Understanding controlled drug release from mesoporous silicates: theory and experiment, J. Control. Rel 53 (2011) 409–417.

[41]. Lipka J, Semmler-Behnke M, Sperling RA, Wenk A, Takenakaa S, Schleha C, Kisselb T, Parakc WJ, Kreyling WG, Biodistribution of PEG-modified gold nanoparticles following intratracheal instillation and intravenous injection, Biomat. 31 (2010) 6574–6581.

[42]. Nair LS, Laurencin CT, Biodegradable polymers as biomaterials, Prog. Polym. Sci 32 (2007) 762–798.

[43]. Kreyling WG, Abdelmonem AM, Ali Z, Alves F, Geiser M, Haberl N, Hartmann R, Hirn S, de Aberasturi DJ, Kantner K, Khadem-Saba G, Montenegro JM, Rejman J, Rojo T, de Larramendi IR, Ufartes R, Wenk A, Parak WJ, In vivo integrity of polymer-coated gold nanoparticles, Nat. Nanotechnol 10 (2015) 619–623. [PubMed: 26076469]

[44]. Shiraishi K, Kawano K, Minowa T, Maitani Y, Yokoyama M, Preparation and in vivo imaging of PEG-poly L-lysine-based polymeric micelle MRI contrast agents, J. Control Rel 136 (2009) 14–20.

[45]. Zhang X, Wu D, Shen X, Liu P, Fan F, Fan S, In vivo renal clearance, biodistribution, toxicity of gold nanoclusters, Biomat 33 (2012) 4628–4638.

[46]. Guo Y, Chen WJ, Wang WW, Shen J, Guo RM, Gong FM, Lin SD, Cheng D, Chen GH, Shuai XT, Simultaneous diagnosis and gene therapy of immunorejection in rat allogeneic heart transplantation model using a T cell-targeted theranostic nanosystem, ACS Nano 6 (2012) 10646–10657. [PubMed: 23189971]

[47]. Kim C, Favazza C, Wang LV, In vivo photoacoustic tomography of chemicals:high-resolution functional and molecular optical imaging at new depths, Chem. Rev 110 (2010) 2756–2782. [PubMed: 20210338]

[48]. Huang J, Guo M, Ke H, Zong C, Ren B, Liu G, Shen H, Ma Y, Wang X, Zhang H, Rational design and synthesis of cFe2O3@Au magnetic gold nanoflowers for efficient cancer theranostics, Adv. Mater 34 (2015) 5049–5056.

[49]. Wang H, Liu C, Gong X, Hu D, Lin R, Sheng Z, Zheng C, Yan M, Chen J, Cai L, In vivo photoacoustic molecular imaging of breast carcinoma with folate receptortargeted indocyanine green nanoprobes, Nanoscale 6 (2014) 14270–14290.

[50]. Kakizawa Y, Furukawa S, Kataoka K, Block copolymer-coated calcium phosphate nanoparticles sensing intracellular environment for oligodeoxynucleotide and siRNA delivery, J. Control Rel 97 (2004) 345–356.

[51]. Piella J, Bastus NG, Puntes V, Size-controlled synthesis of sub-10-nanometer citrate-stabilized gold nanoparticles and related optical properties, Chem. Mater 28 (2016) 1066–1075.

[52]. Matsumoto Y, Nichols JW, Toh K, Nomoto T, Cabral H, Miura Y, Christie RJ, Yamada N, Ogura T, Kano MR, Vascular bursts enhance permeability of tumour blood vessels and improve nanoparticle delivery, Nat. Nanotechnol 11 (2016) 533–538. [PubMed: 26878143]

[53]. Li L, ten Hagen TLM, Bolkestein M, Gasselhuber A, Yatvin J, van Rhoon GC, Eggermont AMM, Haemmerich D, Koning GA, Improved intratumoral nanoparticle extravasation and penetration by mild hyperthermia, J. Control Rel 167 (2013) 130–137.

[54]. Sahu P, Bhatt A, Chaurasia A, Gajbhiye V, Enhanced hepatoprotective activity of piperine loaded chitosan microspheres, Int. J. Drug Dev. Res 4 (2012) 259–262.

[55]. Yadav S, Sahu P, Chaurasia A, Role of Cyamopsis tetragonoloba against Cisplatin induced Genotoxicity: Analysis of Micronucleus and Chromosome Aberrations In vivo, Int. J. Bio Innov 2 (2013) 184–193.

[56]. Das D, Chaurasia A, Sahu P, Mishra VK, Kashaw SK, Antihypercholestrolemic Potential of Omega-3-Fatty Acid Concentrate in Alloxan Induced Diabetic Rodent, Int. J. Pharma. Sci. Res 6 (2015) 3634–3640.

[57]. Chaurasia A, Das D, Sahu P, Evaluation, Assessment & Screening of Antidiabetic Activity of Stevia Rebaudiana leaves extract in Alloxan-Induced Diabetic Rat Model, J. Int. Res. Medical Pharma. Sci 9 (2016) 107–112.

[58]. Vishwakarma APS, Vishwe A, Sahu P, Chaurasia A, Screening of Hepatoprotective Potential of Ethanolic and Aqueous Extract of Terminalia Arjuna Bark against Paracetamol/CCl4 Induced Liver damage in Wistar Albino Rats, Int. J. Pharma. Archive 3 (2013) 1–8.

[59]. Melamed JR, Edelstein RS, Day ES, Elucidating the fundamental mechanisms of cell death triggered by photothermal therapy, ACS Nano 9 (2015) 6–1. [PubMed: 25590560]

[60]. Arunachalam B, Phan UT, Geuze HJ, Cresswell P, Enzymatic Reduction of Disulfide Bonds in Lysosomes: Characterization of a Gamma-Interferon-Inducible Lysosomal Thiol Reductase GILT, P. Natl. Acad. Scie. USA 97 (2000) 745–750.

[61]. Phan UT, Cresswell B, Arunachalam P, Gamma-Interferon-Inducible Lysosomal Thiol Reductase GILT Maturation, Activity, and Mechanism of Action, J. Biol. Chem 275 (2000) 25907–25914.

[62]. Goncalves M, Maciel D, Capelo D, Xiao S, Sun W, Shi X, Rodrigues J, Tomas H, Li Y, Dendrimer-Assisted Formation of Fluorescent Nanogels for Drug Delivery and Intracellular Imaging, Biomacromolecules. 15 (2014) 492–499. [PubMed: 24432789]

[63]. Wang YXJ, Hussain SM, Krestin GP, Superparamagnetic Iron Oxide Contrast Agents: Physicochemical Characteristics and Applications in MR Imaging, Eur. Radiol 11 (2001) 2319–2331. [PubMed: 11702180]

[64]. Velpandian T, Bankoti R, Humayun S, Ravi AK, Kumari SS, Biswas NR, Comparative evaluation of possible ocular photochemical toxicity of fluoroquinolones meant for ocular use in experimental models, Indian J. Exp. Biol 44 (2006) 387–391. [PubMed: 16708892]

[65]. Davis SS, Hardy JG, Newman SP, Wilding IR, Gamma scintigraphy in the evaluation of pharmaceutical dosage forms, Eur. J. Nucl. Med 19 (1992) 971–986.

[66]. Gorczyca G, Tylingo R, Szweda P, Augustin E, Sadowska MS Milewski, Preparation and characterization of genipin crosslinked porous chitosan collagen gelatin scaffolds using chitosan-CO2 solution, Carbohydr. Polym 102 (2014) 901–911. [PubMed: 24507362]

[67]. Berger J, Reist M, Mayer JM, Felt O, Peppas NA, Gurny R, Structure and interactions in covalently and ionically crosslinked chitosan hydrogels for biomedical applications, Eur. J. Pharm. Biopharm 57 (2004) 19–34. [PubMed: 14729078]

[68]. Mortazavi SA, Smart JD, An Investigation in to the role of water movement and mucus gel dehydration in mucoadhesion, J. Control rel 25 (1995) 197–203.

[69]. Sorlier P, Rochas C, Morfin I, Viton C, Domard A Light Scattering Studies of the Solution Properties of Chitosans of Varying Degrees of acetylation, Biomacromolecules 4 (2003) 1034–1040. [PubMed: 12857089]

[70]. Ravi Kumar MNV, Chitosan chemistry and pharmaceutical perspectives, Chemical Reviews 104 (2004) 6017–6084. [PubMed: 15584695]

[71]. Jin J, Song M, Hourston DJ, Novel chitosanbased films cross459 linked by genipin with improved physical properties, Biomacromolecules 5 (460) (2004) 162–168. [PubMed: 14715022]

[72]. Signini R, Campana Filho SP, On the preparation and characterization of chitosan hydrochloride, Polymer Bulletin 42 (1999) 159–166.

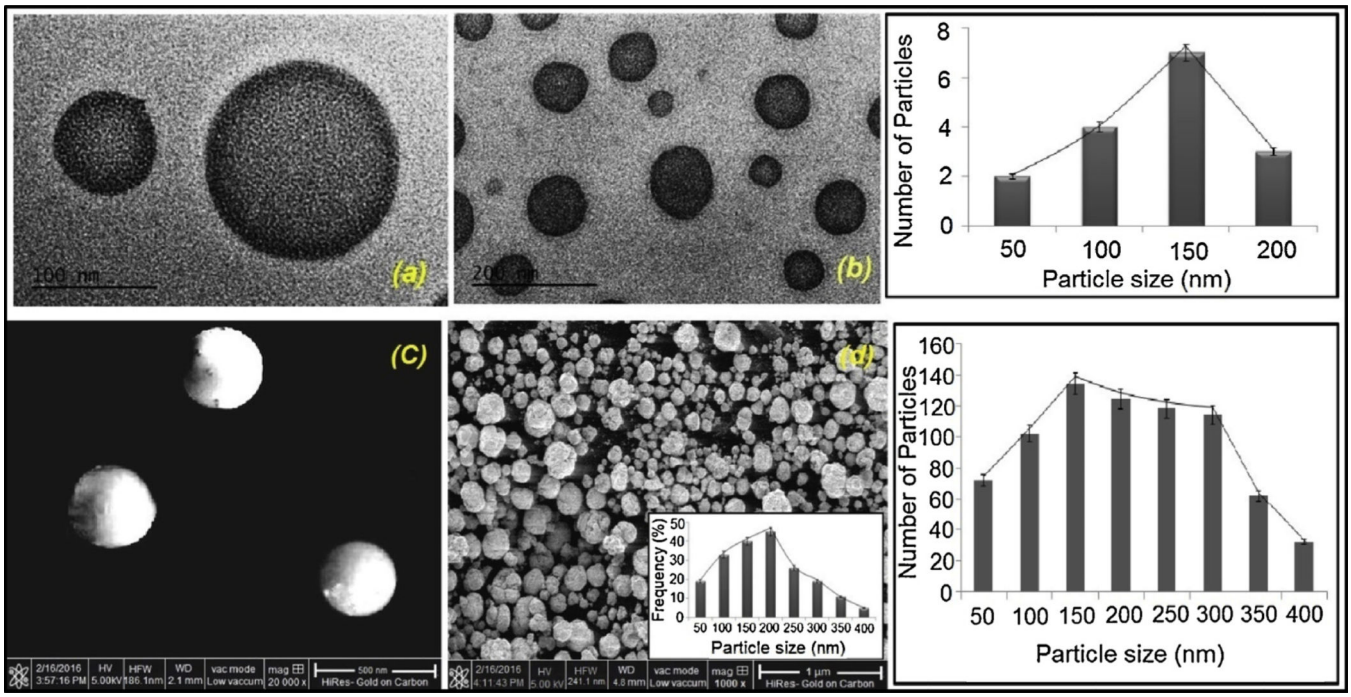

Fig. 1.

Electron micrographs of 5-FU Chitosan Nanogel at different magnificaitons are shown (a) TEM, scale bar = 100nm and; (b) TEM, scale bar = 200nm (c) SEM scale bar = 500 nm; and (d) SEM, scale bar = 1 μm. The particle size histograms are also shown on the right. (Mean+ SD, n = 3).

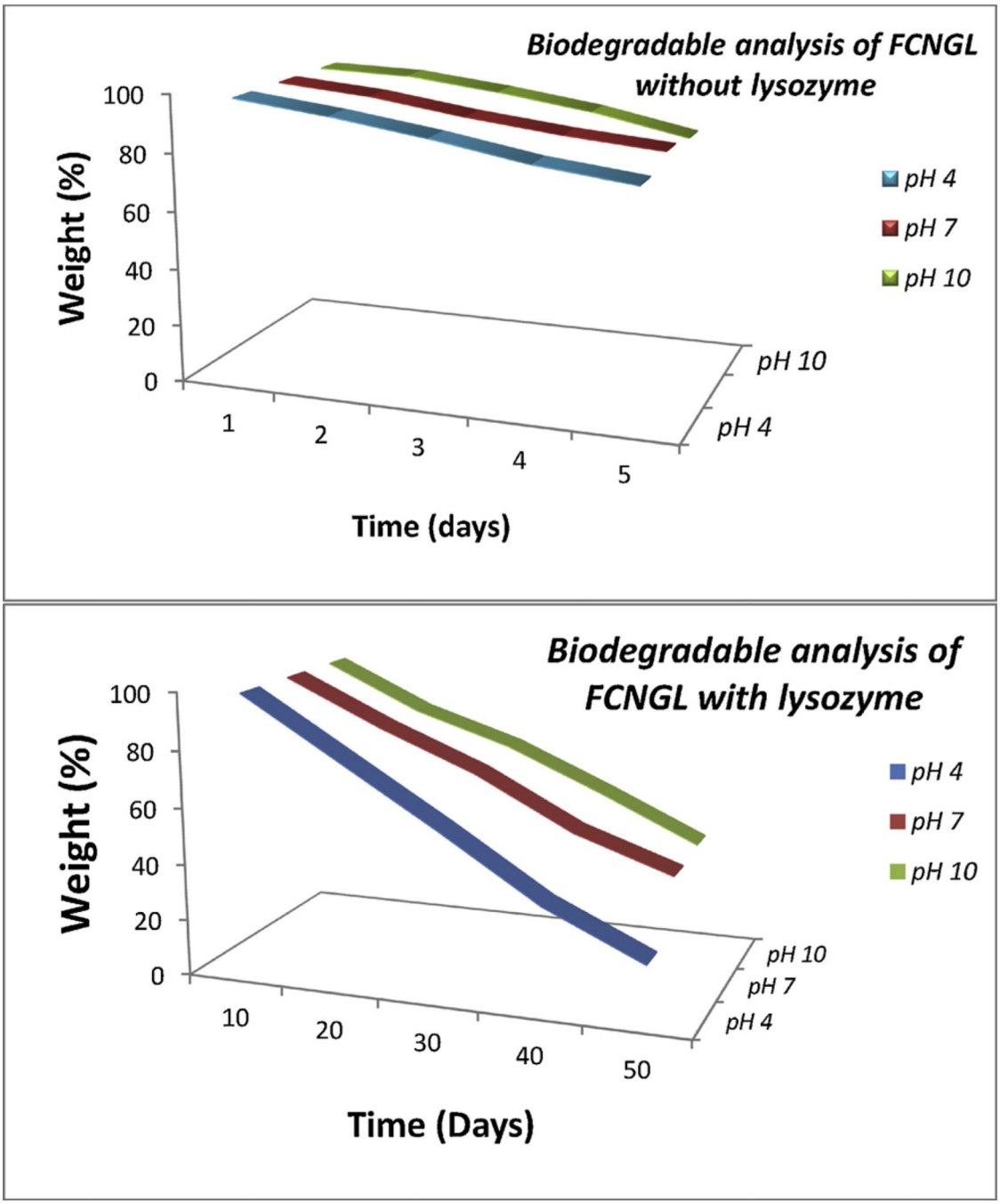

Fig. 2.

The biodegradation assay of 5-FU chitosan nanogel with and without lysozyme at different pH range are shown (Mean+ SD, n =3).

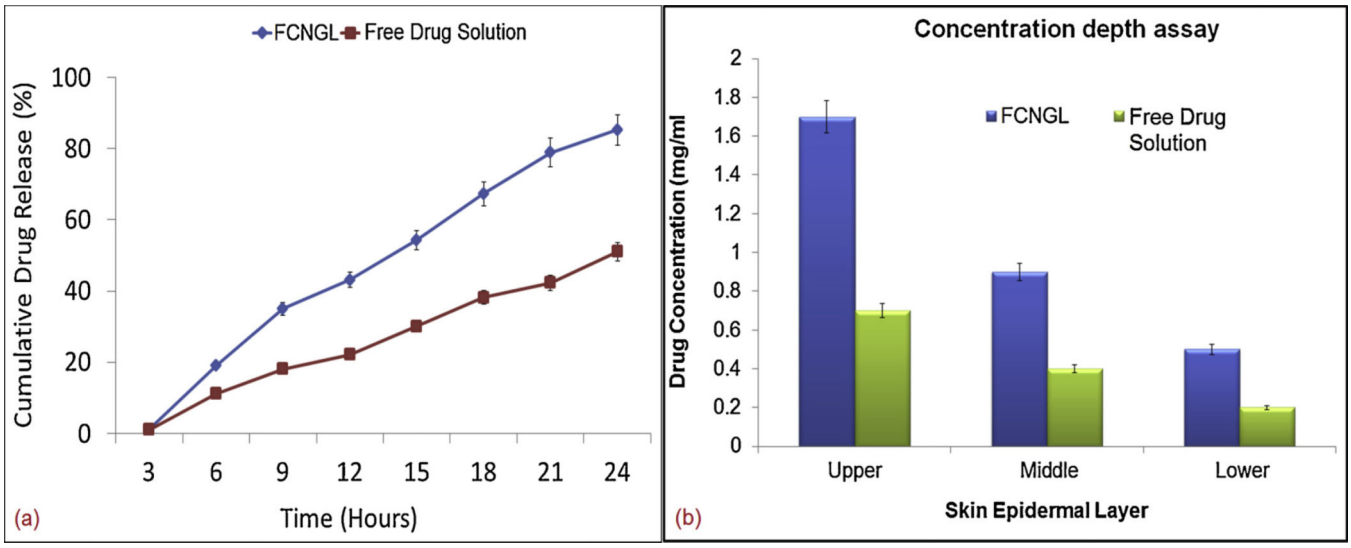

Fig. 3.

Demonstration of ex-vivo penetration profile of FCNGL depicting (a) steady state flux measurement and (b) drug concentration depth evaluation at various epidermal leyers of porcine tissue on 24 h of experimental exposure, (Mean+ SD, n = 3).

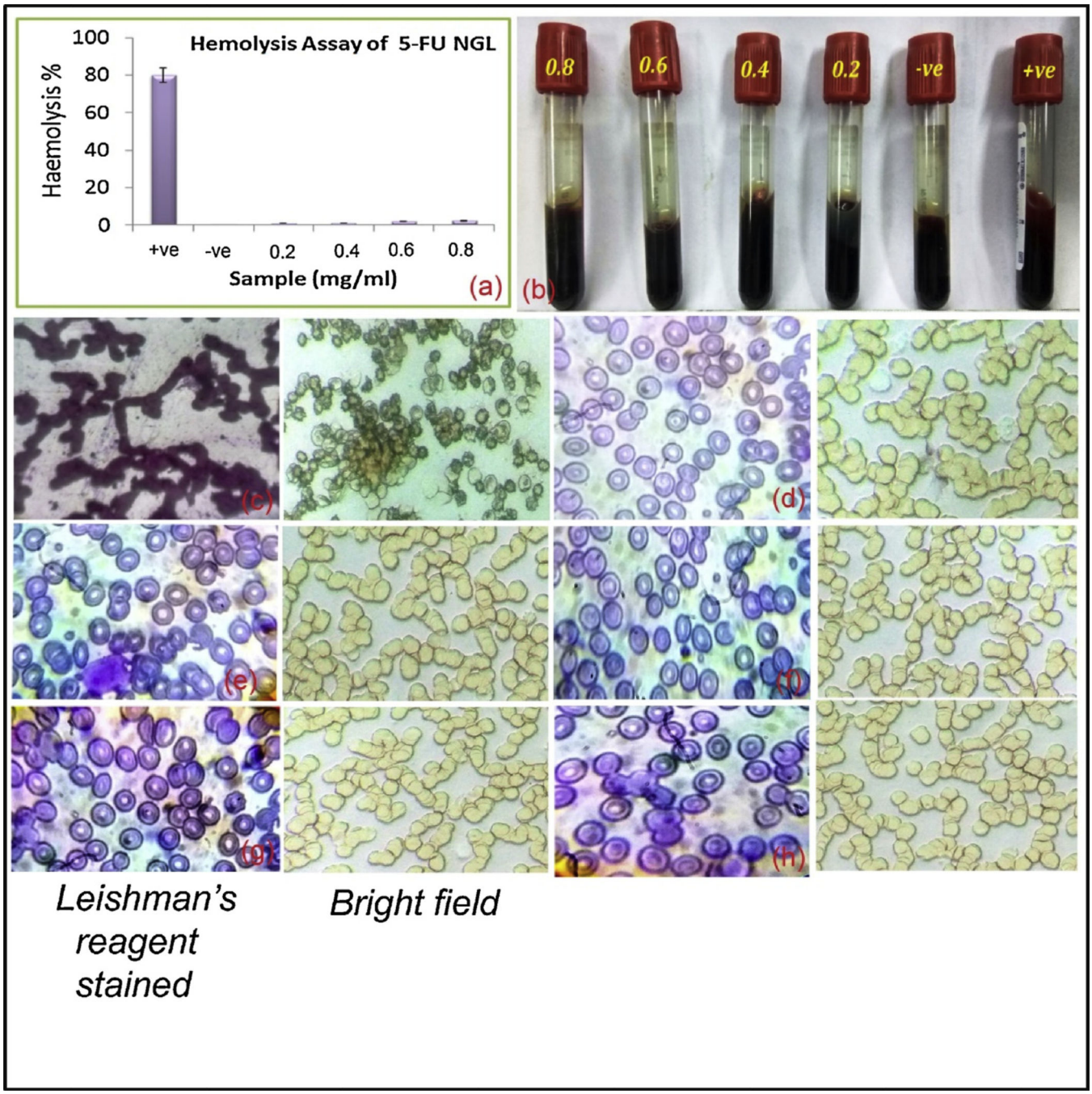

Fig. 4.

Image a & b shows hemolysis ratio analysis of FCNGL at various concentration of blood (0.2 – 0.8 mg/ml). Image c-h (were c = positive control, d = negative control, e = 0.2 mg/ml, f = 0.4, g = 0.6 and h = 0.8 mg/ml of FCNGL) demonstrates microscopic analysis of blood smear slide stained with 1 % w/v Leishman's reagent and visualized at 100X magnification or images captured in bright field at 40X magnification using light microscope (Olympus, Japan). The data exhibit no rupture of RBCs in FCNGL treated group, (Mean + SD, n = 3).

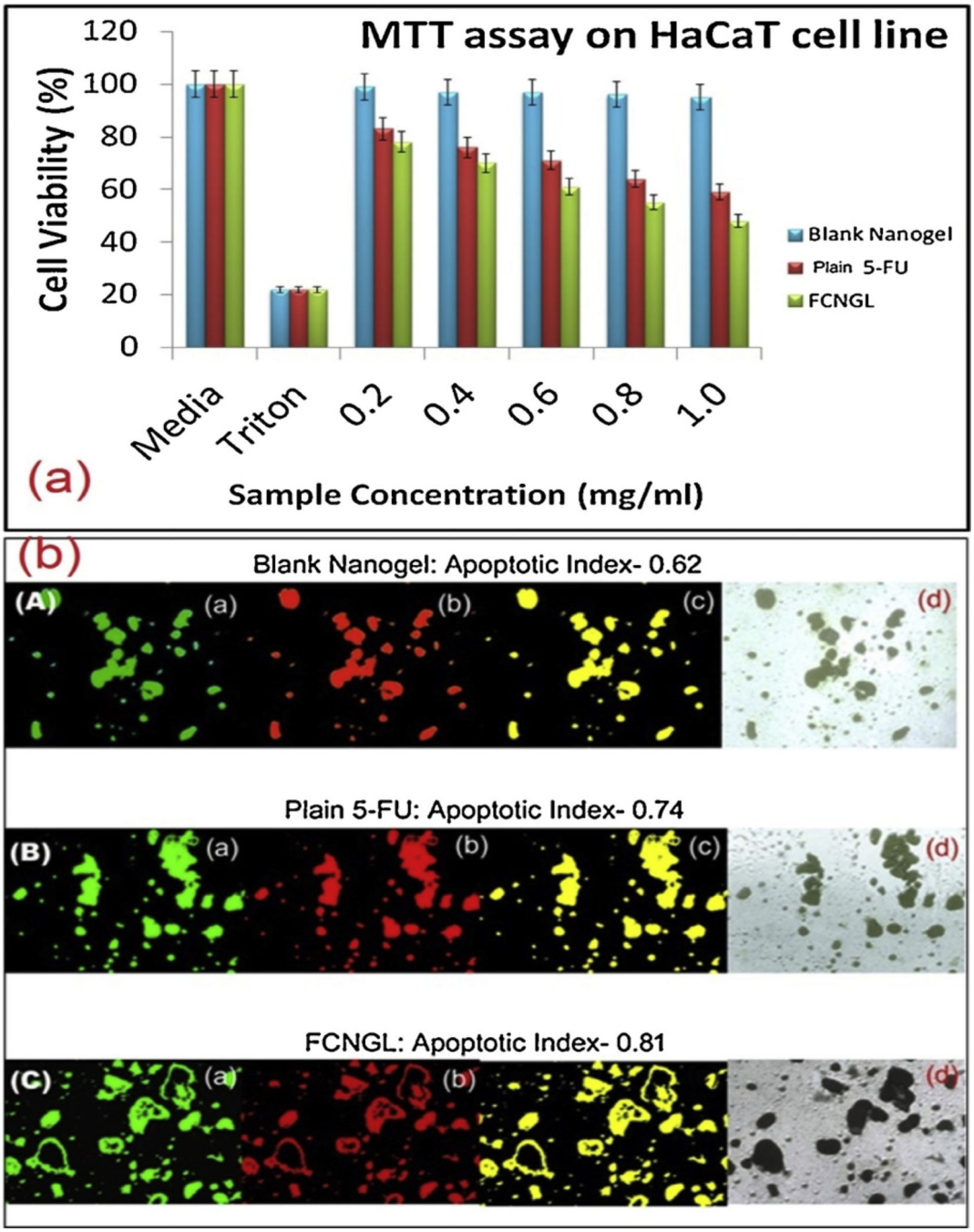

Fig. 5.

(a) Cytotoxicity assay (MTT) on HaCaT cell line by different samples (mean +SD, n = 3), *p < 0.05 and *p < 0.01compared to the untreated cell are shown, (b) Apoptosis assay of (A) blank nanogel (10 μg/ml; 6 h incubation) and (B) plain 5-FU solution (equivalent to 10 μg/ml and incubated for 6 h) (C) FCNGL (equivalent to 10 μg/ml and incubated for 6 h) against HaCaT cells are shown; (a) Green channel depicts the fluorescence from carboxy fluorescein (cell viability marker dye); (b) Red channel depicts fluorescence from Annexin Cy3.18 conjugate (cell apoptosis marker dye); (c) Overlay image of figure (a) and figure (b);

whereas, (d) Depicts the differential contrast image (DIC) of representative cells. The apoptosis index measured as ratio of fluorescence intensity from the red channel to that of green channel. The fluorescence intensities of the images were measured using Image J software, U. S. National Institutes of Health, Bethesda, Maryland, USA, http://imagej.nih.gov/ij/.

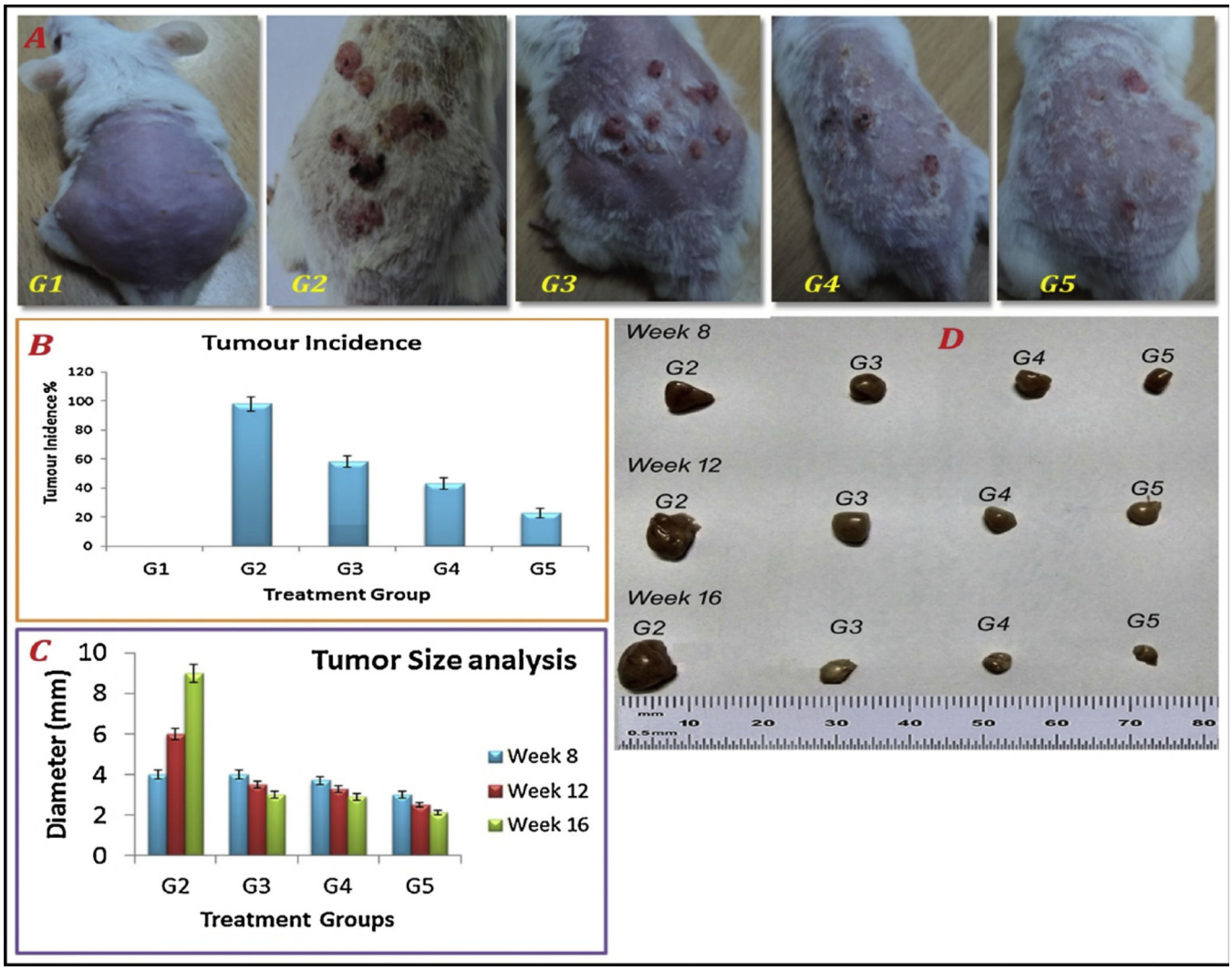

Fig. 6.

Melanoma growth regression study in mice models: (A) representative non-tumor bearing mice healthy control (G1); tumor bearing mice control without treatment (G2); tumor bearing mice treated with 5% w/v marketed 5-FU formulation (G3), and tumor bearing mice treated with FCNGL (0.1% w/v) (G4) and 0.2% w/v (G5) are shown; (B) tumor incidence summary of all treatment and control mice are shown. (C) Tumor diameter profile of different treatment and untreated group, and (D) representative excised tumor after 8 wks., 12 wks., 16 wks. of post-treatment of G2, G3, G4 and G5 evaluated in millimetre scale are shown ($p < 0.05$, $n = 6$).

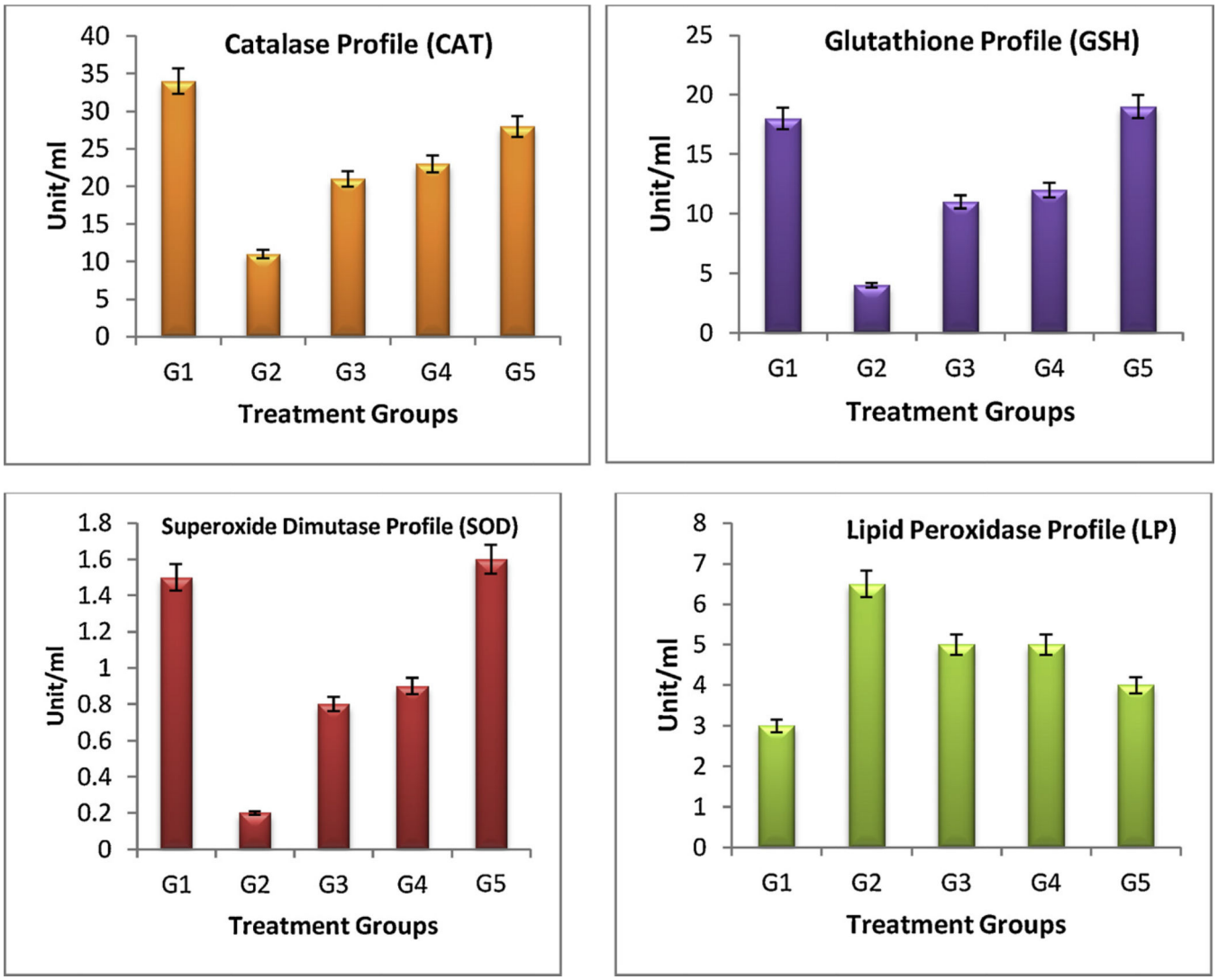

Fig. 7.

Blood biochemical parameters analysis of control (G1 & G2) and treatment (G3-G5) mice is shown. It is observed that mice treated with G4 and G5 have elevated levels of antioxidant enzymes (GTH, CAT and SOD) and lowering of lipid peroxidase (LP) levels when compared to the G2 control and G3 treated formulation, $p < 0.05$, $n = 6$.

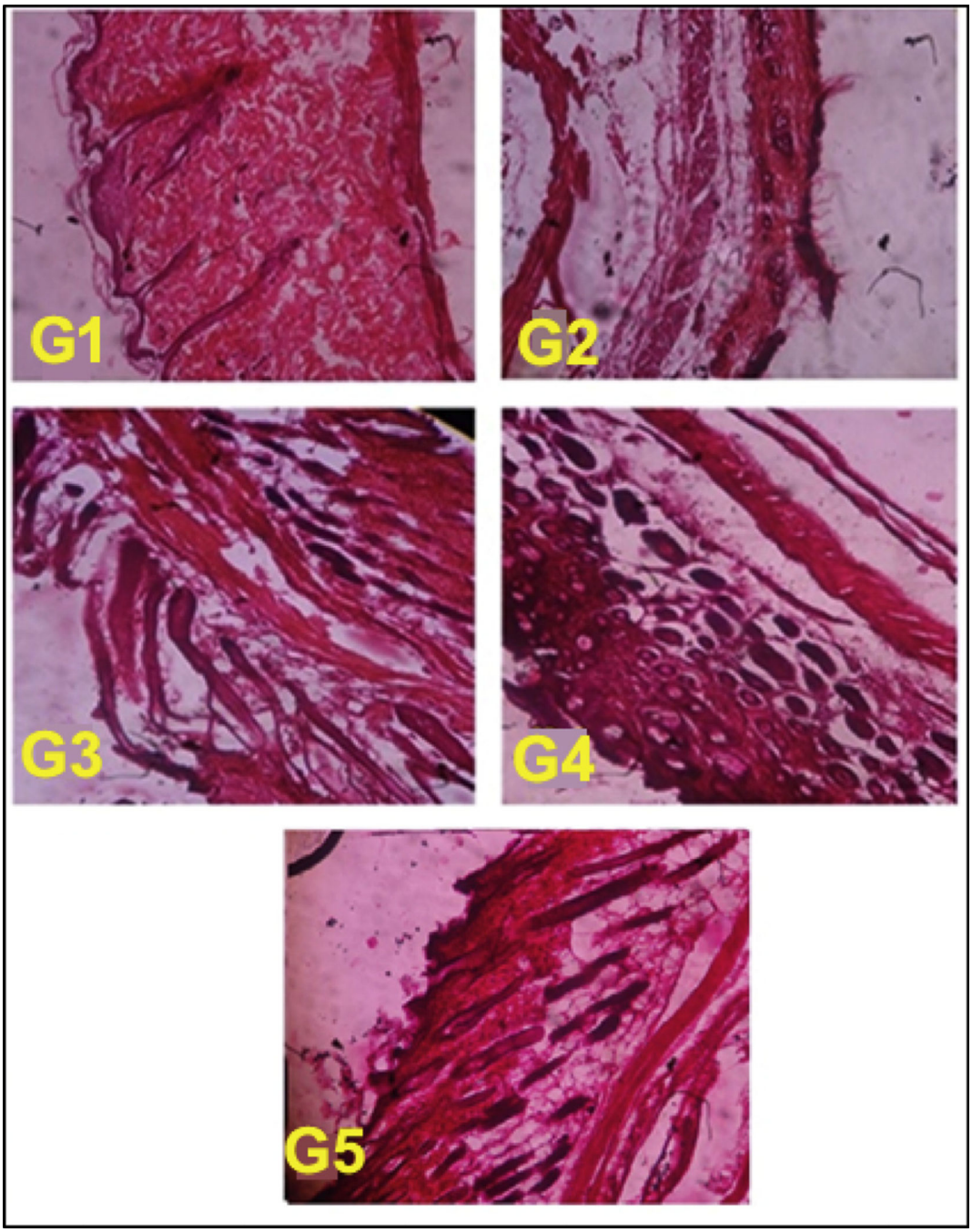

Fig. 8.

Melanoma affected skin histopathology of control (G1-G2) and treatment mice marketed and FCNGL formulation (G3-G5) are shown. The tissue architecture of non-tumor bearing mouse (G1) is well aligned; G2-mouse skin is completely broken with rupture of dermis layer; G3-mouse skin shows some degree of improvement in skin texture; in G4 and G5 treatment mouse, skin histology shows significantly healing with regeneration of keratinized squamous tissue. The tissue was visualized at 100X magnification using light microscope (Olympus, Japan), $p < 0.05$, $n = 6$.

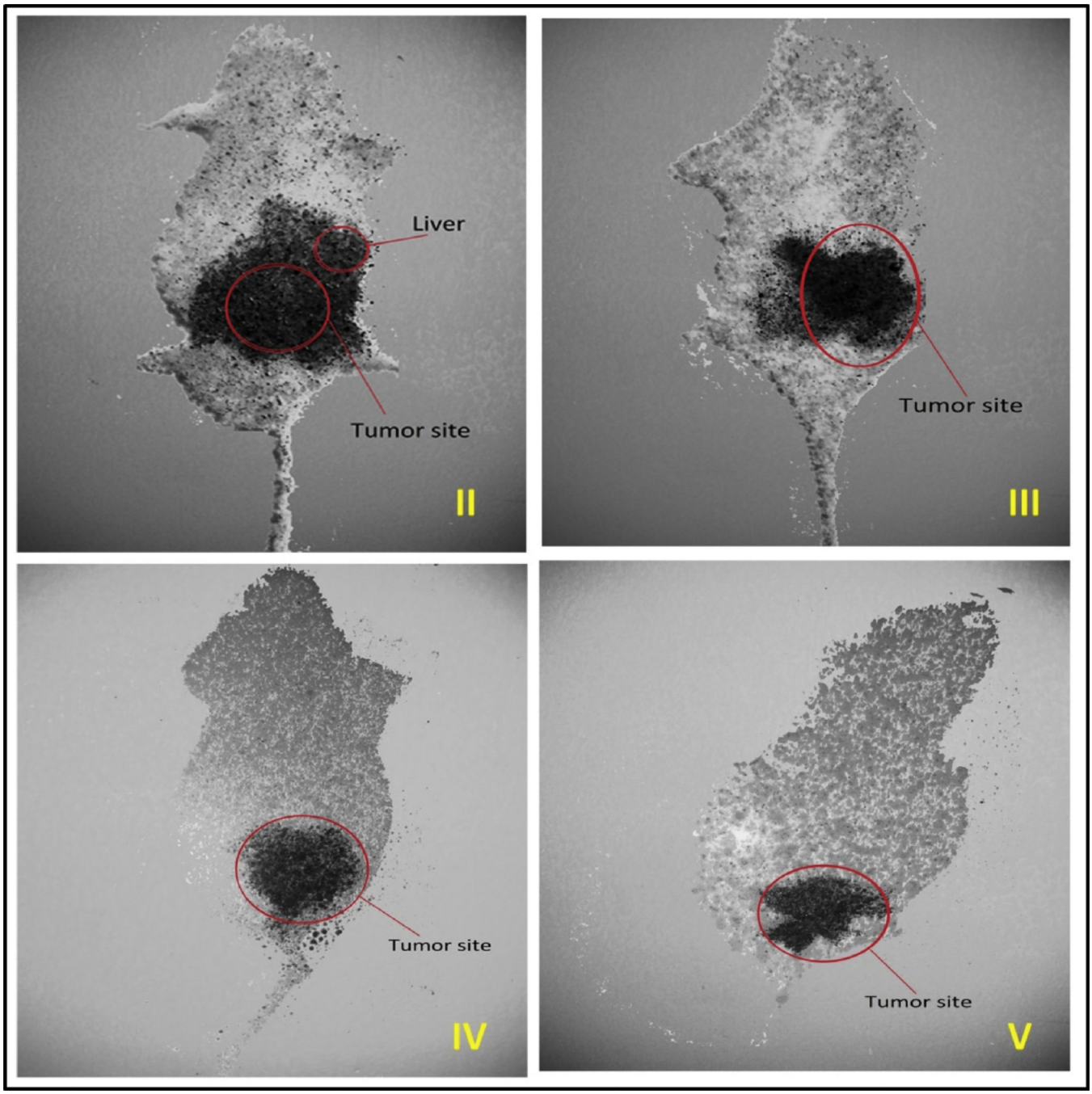

Fig. 9.

Whole body gamma scintigraphic imaging of Swiss albino mice using different treated formulation (G3-G5) against untreated control (G2) is shown. For G4-G5 treatment, ^{99m}Tc localization is significantly localized at tumor site (above right hind leg) with less accumulation in non-specific organs compared with control.

Table 1

Pharmacokinetic profile of radiolabelled 99 m-Tc-FCNGL topical formulation at different time interval in various animal groups (Mean ± SD, n = 3).

S. No.	Formulation	Blood / Tissue	C_{max} (%/g)	T_{max} (h)	AUC $_{0-24}$ (h%/g)	K_{el} (I/h)	$T_{1/2}$ (h)
1.	5% FU gel (**G3**)	Blood	0.29± 0.21	2.56± 0.37	2.95± 0.51	0.28± 0.13	2.11± 0.16
		Skin	58.05± 1.28	0.48± 2.43	399.5± 0.48	0.19± 2.14	5.95± 0.97
2.	0.1% FCNGL	Blood	0.31± 0.01	2.99± 0.15	3.16± 0.57	0.32± 0.66	2.67± 0.09
	(**G4**)	Skin	61.20± 1.63	0.51± 2.57	415.7± 1.31	0.21± 2.04	6.01± 1.33
3.	0.2% FCNGL	Blood	0.33± 0.22	3.06± 0.59	3.21± 0.05	0.31± 0.19	3.0± 0.54
	(**G5**)	Skin	63.3± 2.64	0.53± 2.03	469.7± 1.52	0.22± 1.97	6.00± 1.55